2012

Depositional environments of Upper Meiocene through Pleistocene siliciclastic sediments, Baton Rouge aquifer system, southeastern Louisiana

Elizabeth Laurel Chamberlain
Louisiana State University and Agricultural and Mechanical College, echamb1@tigers.lsu.edu

DEPOSITIONAL ENVIRONMENTS OF UPPER MIOCENE THROUGH PLEISTOCENE SILICICLASTIC SEDIMENTS, BATON ROUGE AQUIFER SYSTEM, SOUTHEASTERN LOUISIANA

A Thesis

Submitted to the Graduate Faculty of the
Louisiana State University and
Agricultural and Mechanical College
in partial fulfillment of the
requirements for the degree of
Master of Science

in

The Department of Geology and Geophysics

by

Elizabeth Laurel Chamberlain
B.S., B.A., B.A., Louisiana State University, 2007
August 2012

AKNOWLEDGEMENTS

I would like to acknowledge the work and support of my advisor, Dr. Hanor. Every day I think about things I learned from him. I received a great deal of support from my other committee members, Dr. Tsai and Dr. Bentley, as well. This research was funded in part by a grant from the US Geological Survey and National Institutes for Water Resources awarded to Dr. Tsai and Dr. Hanor.

John Anderson, director of the Cartographic Information Center at LSU, taught me how to locate my well logs on a map. Wendy Lovelace of the USGS, former Hanor-graduate student Colleen Wendeborn, and Dr. Tsai provided well log images used herein. Fellow graduate students Matt Clark and Miles McCammon helped with the technological aspects of this project.

I would like to thank my husband, Rye Cooper, for his endless support and patience. Finally, I would like to acknowledge my baby boy, Frederick…not because he helped with this thesis, but because I love him so much.

TABLE OF CONTENTS

AKNOWLEDGEMENTS……ii

ABSTRACT……iv

1. INTRODUCTION……1
    1.1 Nature of the scientific problem……1
    1.2 Research approach……4

2. GEOLOGIC SETTING……6
    2.1 Overview of the geology of the Cenozoic Gulf Coastal Plain……6
    2.2. Baton Rouge aquifer system geology……9
    2.3 Faulting in the Baton Rouge aquifer system……9
    2.4 Saltwater encroachment……10

3. METHODS……14
    3.1 Overview……14
    3.2 Evaluation of subsurface geology through cross sections……18
    3.3 Isometric fence diagrams and log curve morphologies……19
    3.4 Sequence stratigraphic setting using lithology-depth curves……19

4. RESULTS……23
    4.1 Evaluation of subsurface geology through cross sections……23
    4.2 Isometric fence diagrams and log curve morphologies……23
    4.3 Sequence stratigraphic setting using lithology-depth curves……33

5. DISCUSSION……36
    5.1 Baton Rouge aquifer stratigraphy……36
    5.2 Baton Rouge aquifer sand morphologies……37
    5.3 Potential forcing agents……40
    5.4 The influence of sea-level change on lithology……41

6. CONCLUSIONS……49
    6.1 Depositional environments of the Baton Rouge aquifer system……49
    6.2 Applications of this study……49
    6.3 Future work……50

REFERENCES CITED……51

APPENDIX A: WELL LOG INFORMATION……55

APPENDIX B: LITHOLOGY-DEPTH CURVES……61

VITA……66

ABSTRACT

Saltwater encroachment northward into freshwater sands of the Baton Rouge aquifer system, southeast Louisiana, poses a serious environmental threat to the metropolitan water source. The aquifer consists of a 0.6 mile-thick succession of interbedded, unconsolidated south-dipping siliciclastic sandy units and confining mudstones dating from the Upper Miocene through the Pleistocene. The study area is crosscut by the Baton Rouge fault, a west-east trending listric fault that serves as a leaky barrier to saltwater intrusion from the south. A better understanding of the connectivity, morphology and depositional setting of this aquifer system and hydraulic properties of the Baton Rouge fault is necessary for developing strategies to halt or control saltwater intrusion.

This study provides an in-depth geologic evaluation of the depositional environments of these sediments. Seventy five well logs for boreholes located in East Baton Rouge, West Baton Rouge and Livingston parishes provided data for interpreting environments of deposition, correlating sand-rich and mudstone-rich zones, and identifying periods of low and high sediment aggradation. The correlation of units immediately south of the fault provided the basis for a separate study of the permeability architecture of the fault zone. It was concluded that sandy units of the Baton Rouge aquifer system were fluvially deposited and have complex geometries representing channel fill, floodplain, levee and crevasse splay facies. Aquifer sands are interpreted as zones of amalgamated sand bodies deposited during times of low aggradation associated with sea-level falling-stage and lowstand system tracts. The amalgamation created a high degree of connectivity which causes these zones to behave hydraulically like single units. Mudstone-rich sequences are interpreted as having been deposited during times of high aggradation associated with sea-level highstand. Roughly 10 cycles that correlate to USGS-

designated aquifer sands were identified in lithology-depth curves. The number of sandy units is less than the 24 sea-level reversals documented in the northern Gulf of Mexico for the Upper Miocene through the Pleistocene. Fluvial systems are sensitive to changes in relative sea-level up to 400 miles inland but numerous and major unconformities in the study area have removed portions of the geologic record.

1. INTRODUCTION

1.1 Nature of the scientific problem

In the last half century, saltwater encroachment into sands north of the Baton Rouge fault has been identified as a serious environmental threat to drinking water aquifers (Rollo, 1969; Lovelace, 2007; Tsai, 2010). Freshwater aquifers north of the Baton Rouge fault are pumped for industrial, agricultural, irrigation, and aquaculture uses (Sargent, 2007) and are the source of drinking and household water for the Baton Rouge metropolitan area. A better understanding of the hydraulic character, morphology and depositional setting of this aquifer system and the hydraulic properties of the Baton Rouge fault is necessary for developing strategies to halt or control the intrusion of salt water into this drinking water supply (Tsai, 2010).

This study aims to determine the depositional environments of alternating sand and mudstone units that comprise the Baton Rouge aquifer system of southeast Louisiana through the use of well log data from East Baton Rouge (EBR), West Baton Rouge (WBR) and Livingston (LI) parishes (Figure 1.1). This investigation focuses on sediments to a depth of approximately 3,000 feet below the Baton Rouge metropolitan area and includes the units referred to by the USGS as the 400', 600', 800', 1000', 1200', 1500', 1700', 2000', 2400' and 2800' sands (Figure 1.2).

Griffith (2003) presented north-south and west-east cross sections showing freshwater sands, brackish sands, confining clays and fault locations through the study area (Figure 1.2). Griffith's (2003) J-J' cross section showed Baton Rouge aquifer sands as semi-continuous, thick units separated by confining clays and shallowly dipping towards the Gulf of Mexico. Plates in this publication were intended to indicate the locations of potential freshwater sands, and are also highly useful in identifying USGS nomenclature for sand units with depth.

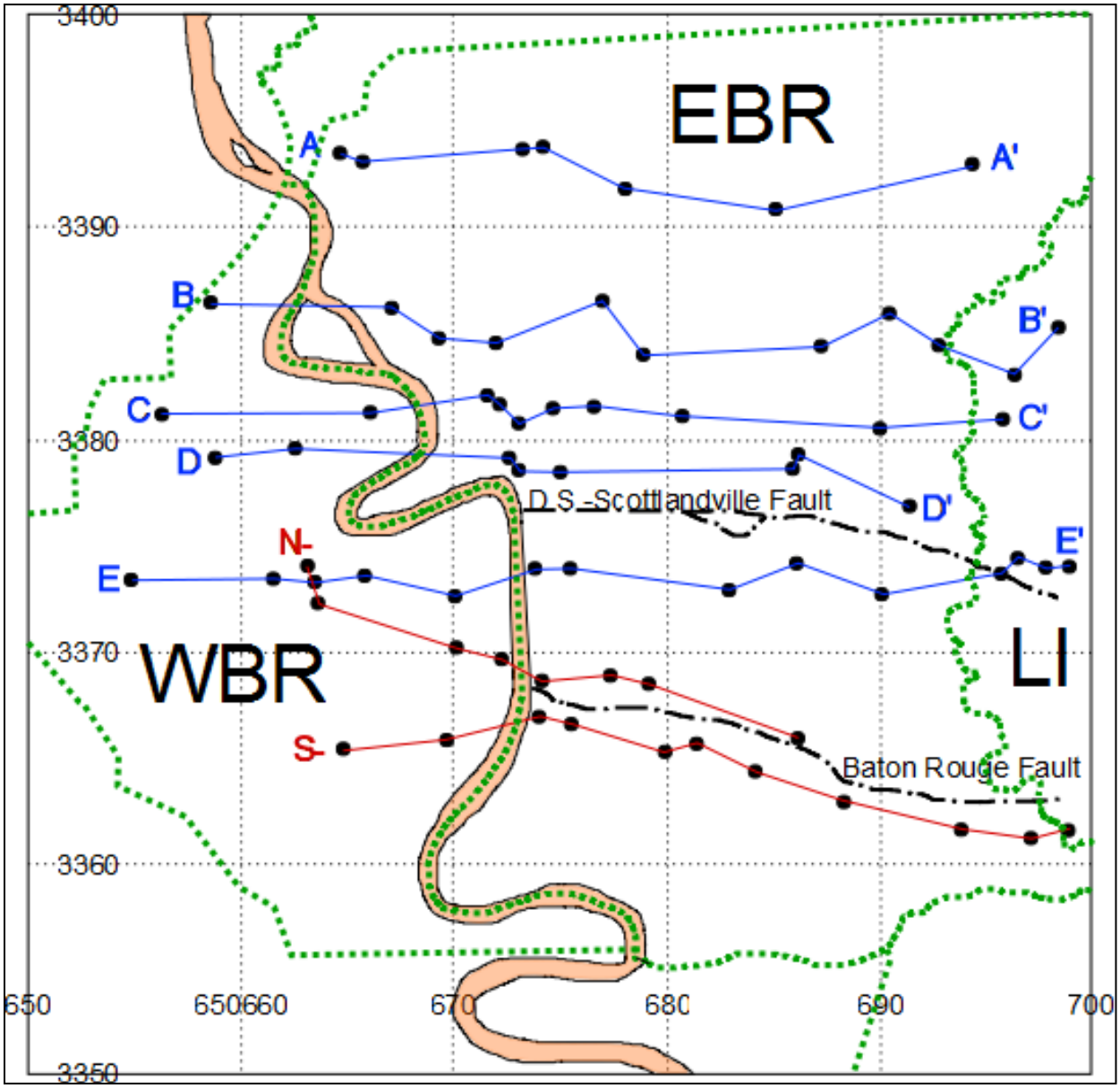

Figure 1.1. The study area is in southeast Louisiana and uses well data from green-shaded parishes including East Baton Rouge (EBR), West Baton Rouge (WBR) and Livingston (LI). The study area includes the modern Mississippi River (shown in brown) and is crosscut by the Baton Rouge and Denham Springs-Scotlandville faults. Transects directly to the north (N-) and south (S-) of the Baton Rouge fault are shown in red. Transects A-A' through E-E' were used to generate lithology-depth curves and are show in blue. Black dots indicate the location of boreholes from which well log data were used. Borehole names and locations are listed in Appendix A. Scale is given in UTM units, Scale is given in UTM units and gridded into 6.21 mile (32,800 feet or 10 kilometer) by 6.21 mile (32,800 feet or 10 kilometer) squares.

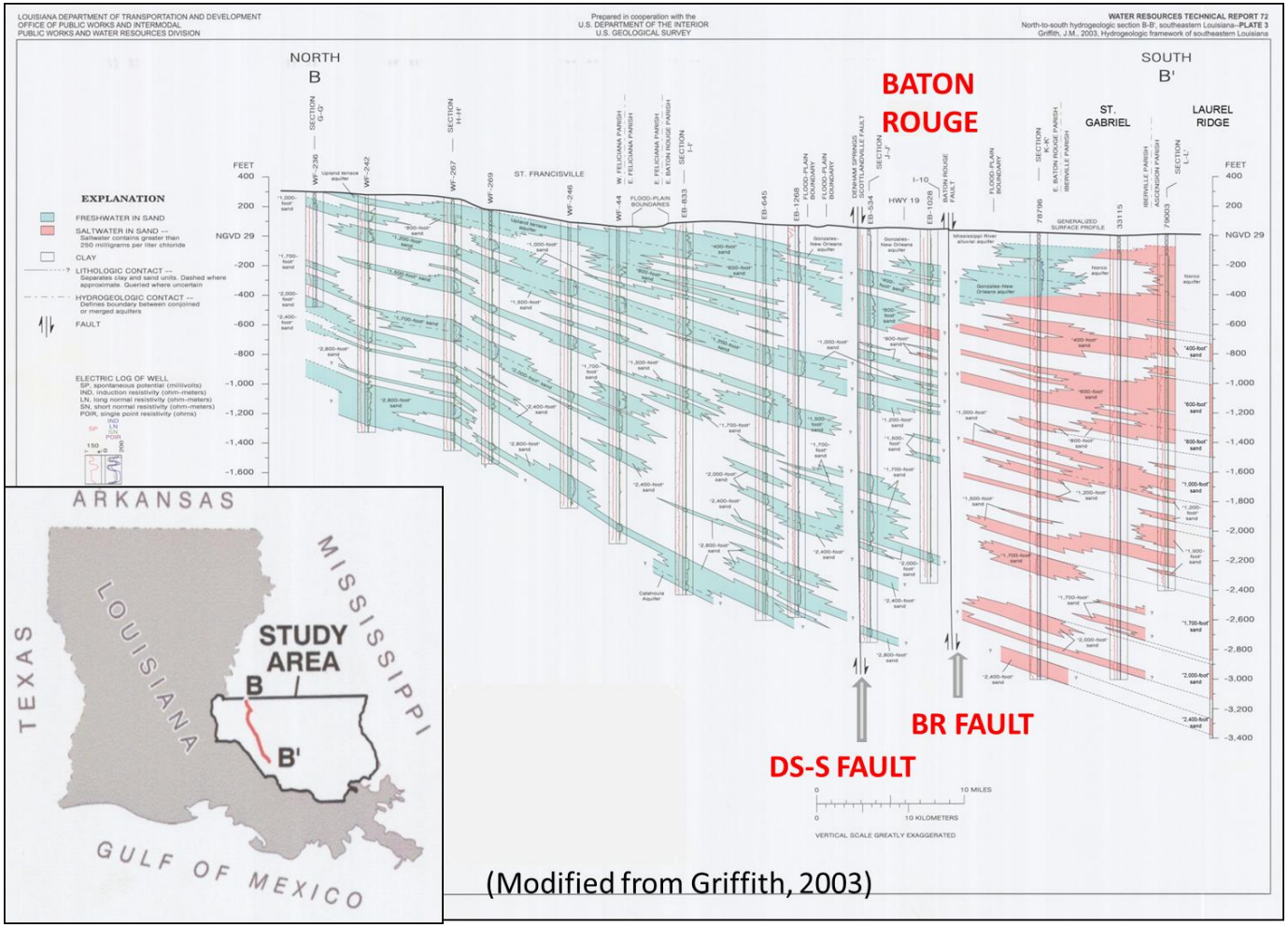

Figure 1.2. North to south cross section which includes the study area and shows USGS-identified aquifer sands, the Denham Springs-Scotlandville (DS-S) and the Baton Rouge (BR) faults modified from Griffith (2003). Freshwater sands are indicated in blue and brackishwater sands are pink. Note large proportion of mudstones (white) and lateral discontinuities in the aquifer units. Note also that the Baton Rouge fault marks the general boundary between freshwater sands to the north and brackish water sands to the south. Pre-development groundwater flow was from north to south.

Work to document saltwater intrusion into the aquifers is noted as early as the mid 1900s. Rollo (1969) presented the first study that showed the complex character of Baton Rouge aquifer sands. Rollo generated four plates showing the 1200', 1500', 2000' and 2400' sands as isometric fence diagrams derived from well log data (Figure 1.3). These plates reflect Rollo's observation that aquifer units vary in thickness. Hanor (1971) used Rollo's diagrams to generate block diagrams that show the sand body morphology (Figure 1.4). The three dimensional renderings by Rollo (1969) and Hanor (1971) suggest highly variable sands.

1.2 Research approach

This research was undertaken to for both scientific and applied purposes. Scientific goals included understanding the basis for the geometry of the Baton Rouge aquifer sands and putting these sediments into a sequence stratigraphic framework. This is important because it provides a geologic basis for the construction and implementation of numerical models of groundwater flow and remediation. While some uncertainty in groundwater models inevitably will exist, too much uncertainty leads to costly remediation designs (Tsai, 2010). Realistic predictions of sand unit morphology and connectivity based on geologic constraints will help to reduce this uncertainty.

It was hypothesized that Baton Rouge aquifer units were deposited by fluvial systems sensitive to external forcing, i.e., the processes and conditions outside the fluvial system that affect deposition. Furthermore, it was proposed that knowledge of the geologic characteristics of these fluvial units is important in understanding pathways of saltwater encroachment in the system.

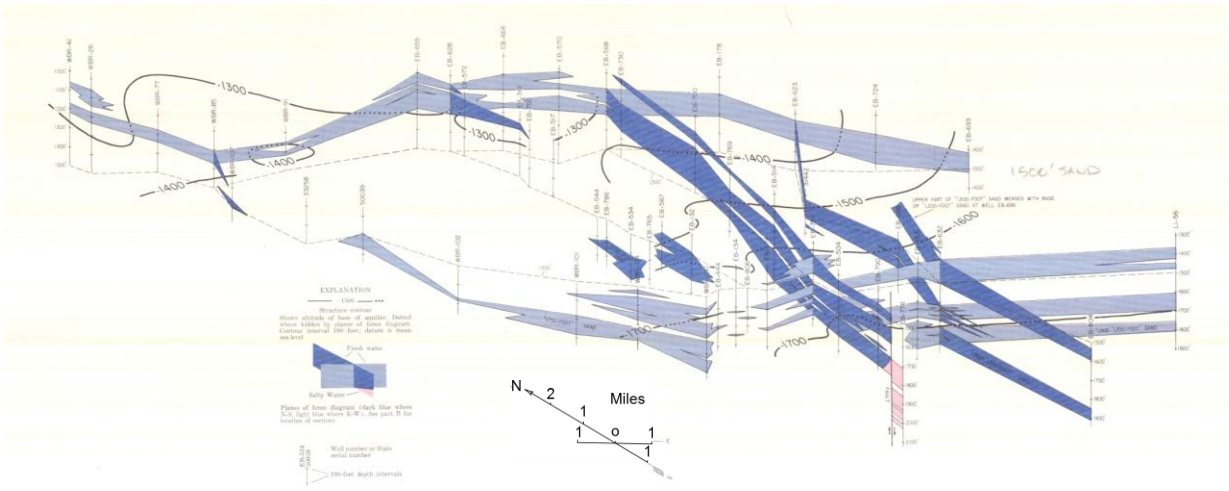

Figure 1.3. Isometric fence diagram for the 1500' sand by Rollo (1969). Complex sand body morphologies are shown including isolated sand lenses and pinched out units.

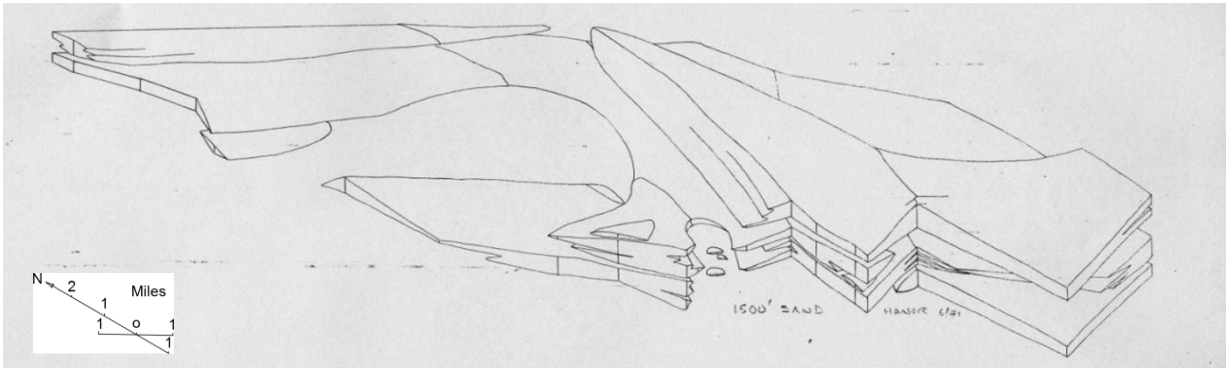

Figure 1.4. Hanor (1971) block diagram for the 1500' sand adapted from Rollo (1969).

2. GEOLOGIC SETTING

2.1 Overview of the geology of the Cenozoic Gulf Coastal Plain

The study area lies in a region which includes sediments of the Louisiana Cenozoic Gulf Coastal Plain. Formation of the Gulf of Mexico began with the breakup of Pangea in the Early to Middle Jurassic (175 Ma) and was complete by 140 Ma (Pindell and Dewey, 1982). This formed a basin which provided accommodation space for sediment deposition. The Cenozoic Gulf Coastal plain is comprised of large, seaward-thickening, wedge-shaped sedimentary complexes composed fluvial, deltaic, and marine sediments (Murray, 1947). These sediments are 20,000 feet or more in thickness. Inland sediments are predominantly fluvial while seaward sediments are predominantly marine (McFarlan and LeRoy, 1988).

The focus of this study is on freshwater-bearing sediments of Upper Miocene through Pleistocene age. According to Galloway (2001) Louisiana Upper Miocene, Pliocene, and Pleistocene deltaic depositional systems were located south of the study area (Figure 2.1) thus making the sediments in the Baton Rouge area fluvial in origin. The ancient Red, Mississippi, and Tennessee rivers were major axes which delivered sediments from Central and Southern Rockies and Southern Appalachian/Cumberland Plateau source areas to the Gulf of Mexico during this time (Galloway, 2005). Of most importance to sediment deposition in southeastern Louisiana were the ancestral Mississippi and Tennessee rivers. The study area lies immediately to the east of the complex fluvial system of the modern Mississippi River (Figure 2.2). Based on interactions between climate, sea-level change and stratigraphy, Blum and Törnqvist (2000) established that global modern (Quaternary) depositional basin systems, including that of the Mississippi River, provide realistic analogues for pre-Quaternary systems on a global scale. Therefore, knowledge of fluvial architecture and controls acting on the modern Mississippi River

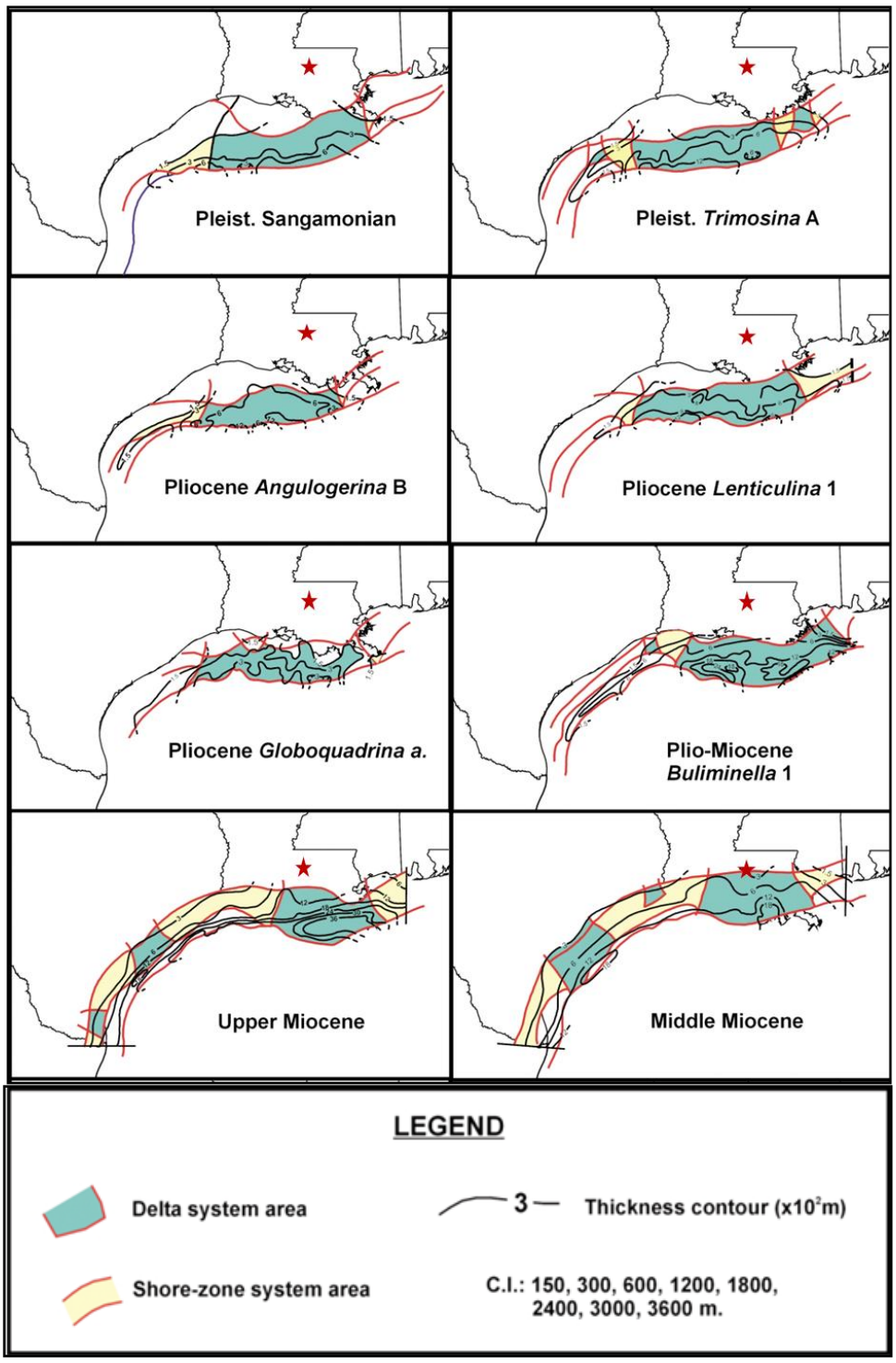

Figure 2.1. Shore-zone and deltaic depositional systems in Upper Miocene to Pleistocene sediments in the northern Gulf of Mexico sedimentary basin (modified from Galloway, 2001). Deltaic depositional systems of the ancestral Mississippi and Tennessee rivers lie to the south of the study area, which is indicated by a red star.

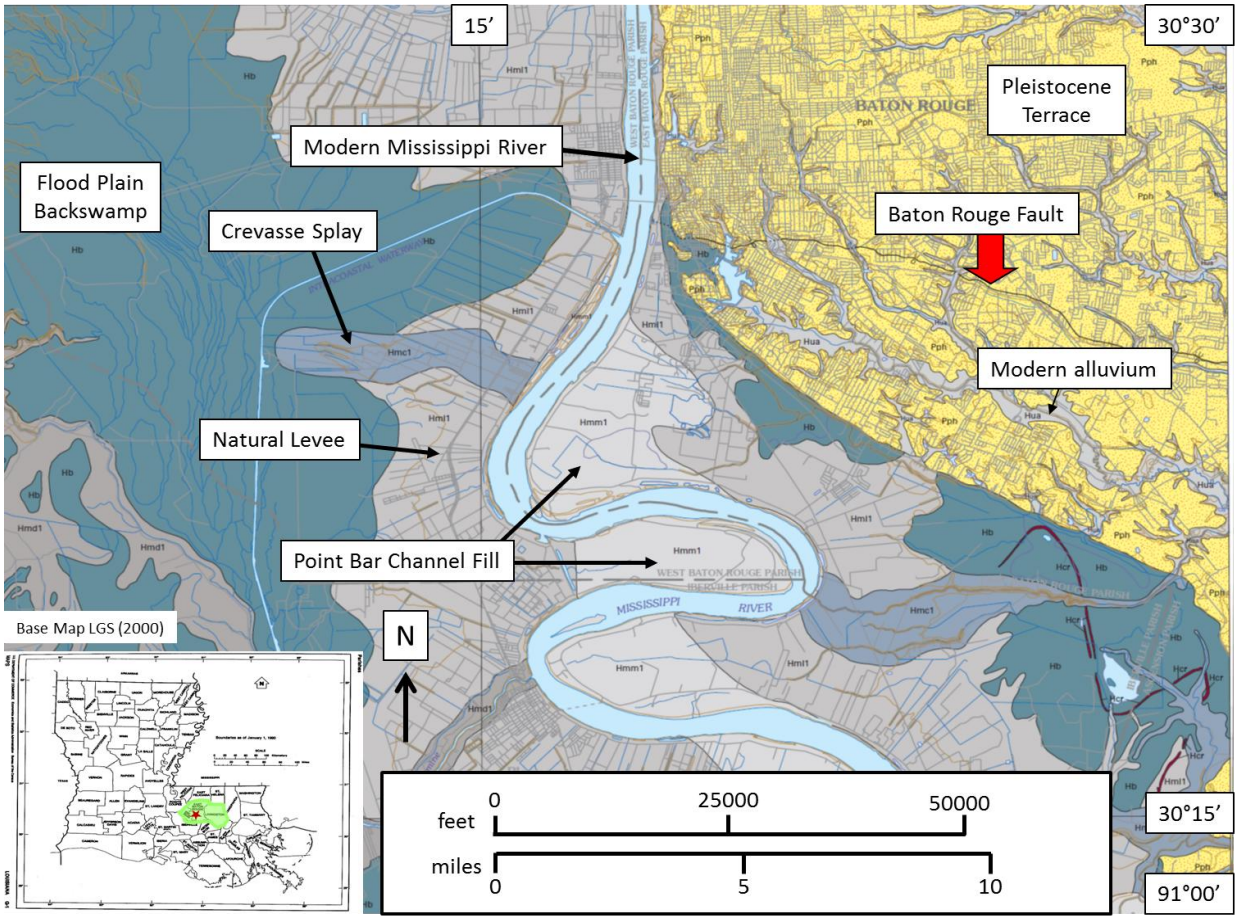

Figure 2.2. The study area is directly to the east of the modern Mississippi river. The surficial geology of the study area is complex and includes the Baton Rouge fault scarp, Pleistocene terraces and natural levee, point bar channel fill, crevasse splay, and floodplain-backswamp deposits. The Denham Springs-Scotlandville fault is directly north of the mapped area.

can be used to help interpret the depositional environments of older southeastern Louisiana Cenozoic sediments.

The USGS recognizes two regional aquifer systems in this area. The Coastal Lowlands aquifer system includes sediments in Louisiana, Mississippi, Alabama, and Florida (Martin and Whiteman, 1989). The Southern Hills aquifer system is specific to southeastern Louisiana and southwestern Mississippi.

2.2 Baton Rouge aquifer system geology

The term Baton Rouge aquifer system is used here informally to represent part of the Southern Hills regional aquifer system (Buono, 1983). The aquifers consist of an approximately 0.6 mile-thick succession of interbedded and unconsolidated siliciclastic sandy units and confining mudstone units that dip toward the south (Martin and Whiteman, 1989). Sediments date in age from the Upper Miocene through the Pleistocene (Table 2.1). The aquifer recharge zone is in southwestern Mississippi and along the Mississippi – Louisiana border and there is topographic gradient favoring groundwater flow to the south (Rollo, 1969). Sandy units of the Baton Rouge aquifer system are named for their approximate depth below ground level in the industrial district in northern Baton Rouge, where there is significant pumping of freshwater for industrial use. The USGS has designated these sands as the 1200' sand, 1500' sand and so on, according to their depth (Griffith, 2003) (Figure 1.2).

2.3 Faulting in the Baton Rouge aquifer system

Two west-east trending listric faults crosscut units of the Baton Rouge aquifer system, the Denham Springs-Scotlandville fault to the north, and the Baton Rouge fault which runs through the metropolitan area (Figure 1.1). McCulloh and Heinrich (2012) found that units south of the Baton Rouge fault are offset by 300 – 350 feet (90 – 107 m). Like many listric growth faults in the region, the Baton Rouge fault was active through the Oligocene after which faulting eased (McCulloh and Heinrich, 2012). The fault became reactivated in the Pleistocene and has likely continued activity though to the present (McCulloh and Heinrich, 2012). Based on Hanor's (1982) evaluation of the analogous Tepetate fault zone, most of the units considered in this study were deposited during a period of fault inactivity.

Table 2.1. USGS-designated sand unit names and ages, Modified from Lovelace and Lovelace (1995).

Age (MA)	System	Series	Baton Rouge Area Aquifers
0			
		Holocene	Shallow sand
	Quaternary		400’ sand
		Pleistocene	600’ sand
1.8			
			800’ sand
			1,000’ sand
		Pliocene	1,200’ sand
			1,500’ sand
			1,700’ sand
	Upper Neogene		
5.3			
			2,000’ sand
			2,400’ sand
			2,800’ sand
		Upper Miocene	
~7 - 10			

2.4 Saltwater encroachment

The Baton Rouge Fault serves as a leaky barrier to saltwater intrusion, with mainly freshwater sands to the north and brackish sands to the south. Anthropogenic withdrawal of waters to the north of the fault has caused migration of brackish water across the fault against the topographically driven gradient into freshwater aquifer units north of the fault (Rollo, 1969) (Figure 2.3). Analysis of well log data by Wendeborn and Hanor (2008) indicated that prior to

1960, freshwater with a salinity of less than 300 mg/L existed to a depths of 2,700 to 3,100 feet (nearly 1km) in aquifer units north of the Baton Rouge fault, with the 2800' sand being the deepest freshwater sand unit. Hypersaline waters are found below that depth (Bray and Hanor, 1990) and are the result of salt dome dissolution (Hanor and Sassen, 1990). Groundwaters south of the fault are largely brackish, with well log-calculated salinities of 1000 to 10,000 mg/L (Wendeborn and Hanor, 2008). Recent saltwater contamination has been seen north of the fault in aquifer units including the 1500' and 2000' sands (Lovelace, 2007). Based on groundwater models developed by Tsai and Li (2008) and Li and Tsai (2009), Tsai (2010) identified a plume of saltwater that was intruding northward in the 1500' sand (Figure 2.4). The flow of this saltwater was caused by excessive withdrawal of water at the Lula pumping wells and by barrier action of the Baton Rouge fault (Tsai, 2010).

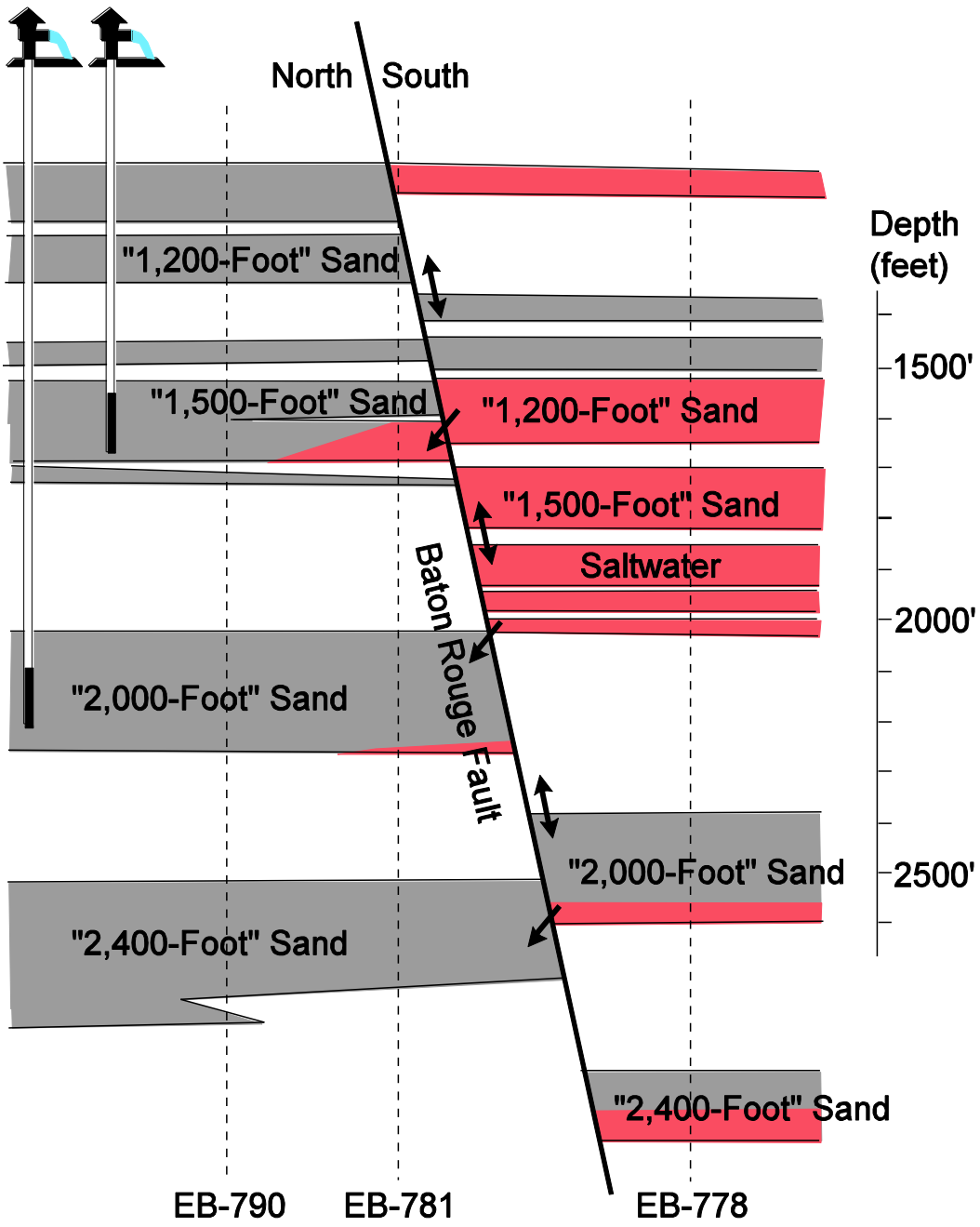

Figure 2.3. Sands north of the Baton Rouge fault contain freshwater that is pumped for industrial, metropolitan and agricultural uses, while waters to the south show elevated salinities. The movement of brackish water into freshwater sand north of the fault has been documented since the mid 1900's (Tsai modified from Rollo, 1969). The south wall of the fault is offset by 300 to 350 feet leading to juxtaposition of aquifer sand units. Borehole names include a parish code and number (e.g. EB-778).

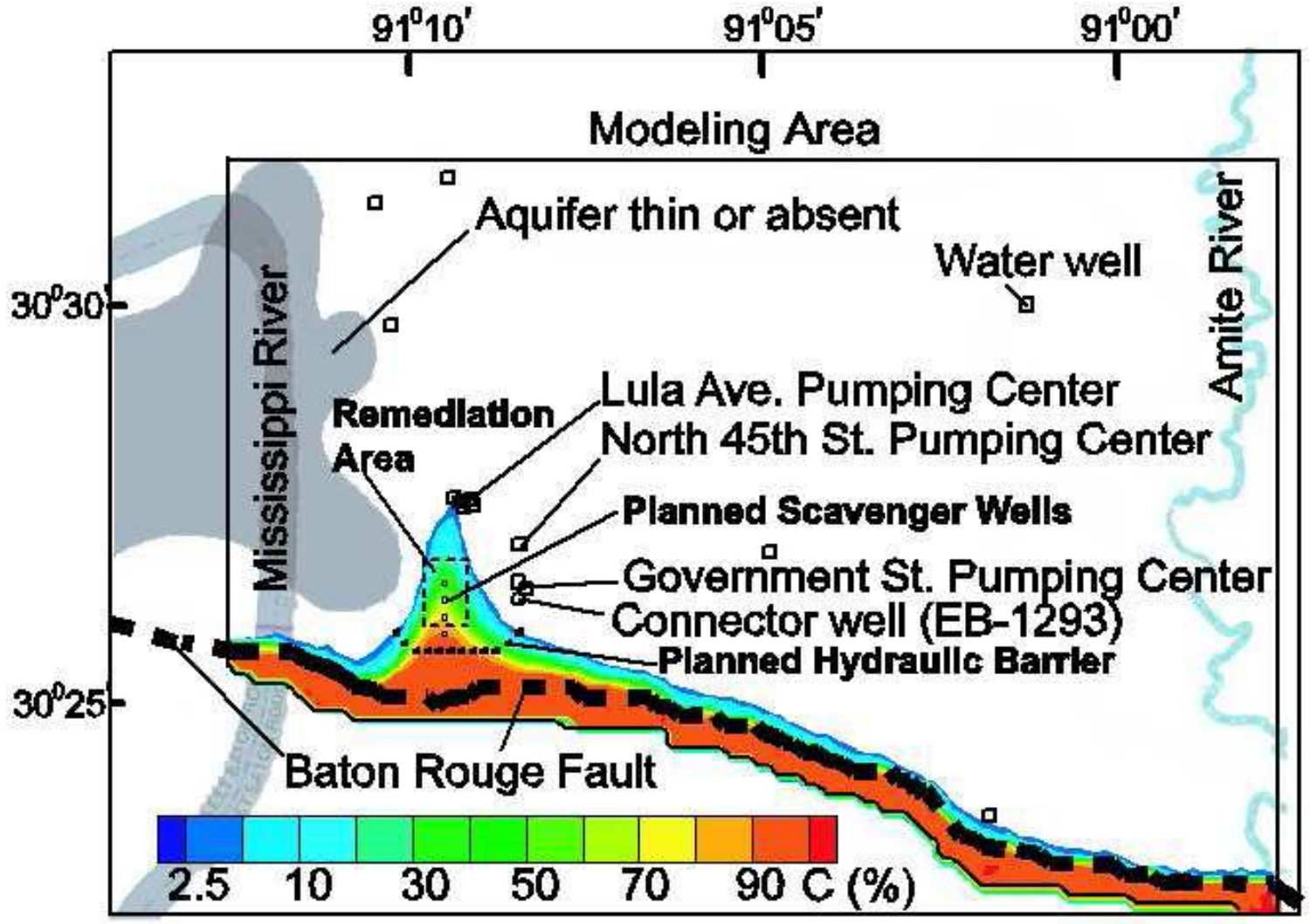

Figure 2.4. Predicted plume of saltwater in January 2005 north of the Baton Rouge fault moving towards the Lula pumping station in the 1500' sand (Tsai, 2010). C (%) is based on the concentration of end-member saltwater present.

3. METHODS

3.1 Overview

The principal sources of information used to establish sandbed geometries and environments of sediment deposition and to identify controls on environments of deposition were wire-line spontaneous potential – resistivity logs for boreholes that had been previous drilled in the study area. A list of these logs and the locations of the boreholes are given in Appendix A. Well log data were used to establish subsurface lithology and to make identifications of depositional facies in the subsurface. While logs have been used for many years in the Baton Rouge area for correlating sand bodies, Paul Heinrich (ca. 1990) in an unpublished report appears to have been the first to use log response to interpret the environments of deposition of sands in the Baton Rouge aquifer system. He identified five log-response facies, two of which he concluded represented deposition by braided streams, two by meandering rivers, and one of unknown origin. He proposed that the braided stream deposits because of their coarser, more uniform character should conduct groundwater better than meandering river deposits.

Seventy five well logs were used in this study which included areas in West Baton Rouge (WBR), East Baton Rouge (EBR) and Livingston (LI) parishes (Figure 1.1). Cross sections immediately north and south of the Baton Rouge fault were drafted from 19 log images used in a previous study (Wendeborn and Hanor, 2008) (Figure 3.1). Resistivity curves were taken from 6 log images provided by Wendy Lovelace from USGS collections and by Frank Tsai (LSU Department of Civil and Environmental Engineering). Frank Tsai provided 50 digital logs derived from Department of Natural Resources SONRIS log images which were used to establish lithology-depth curves.

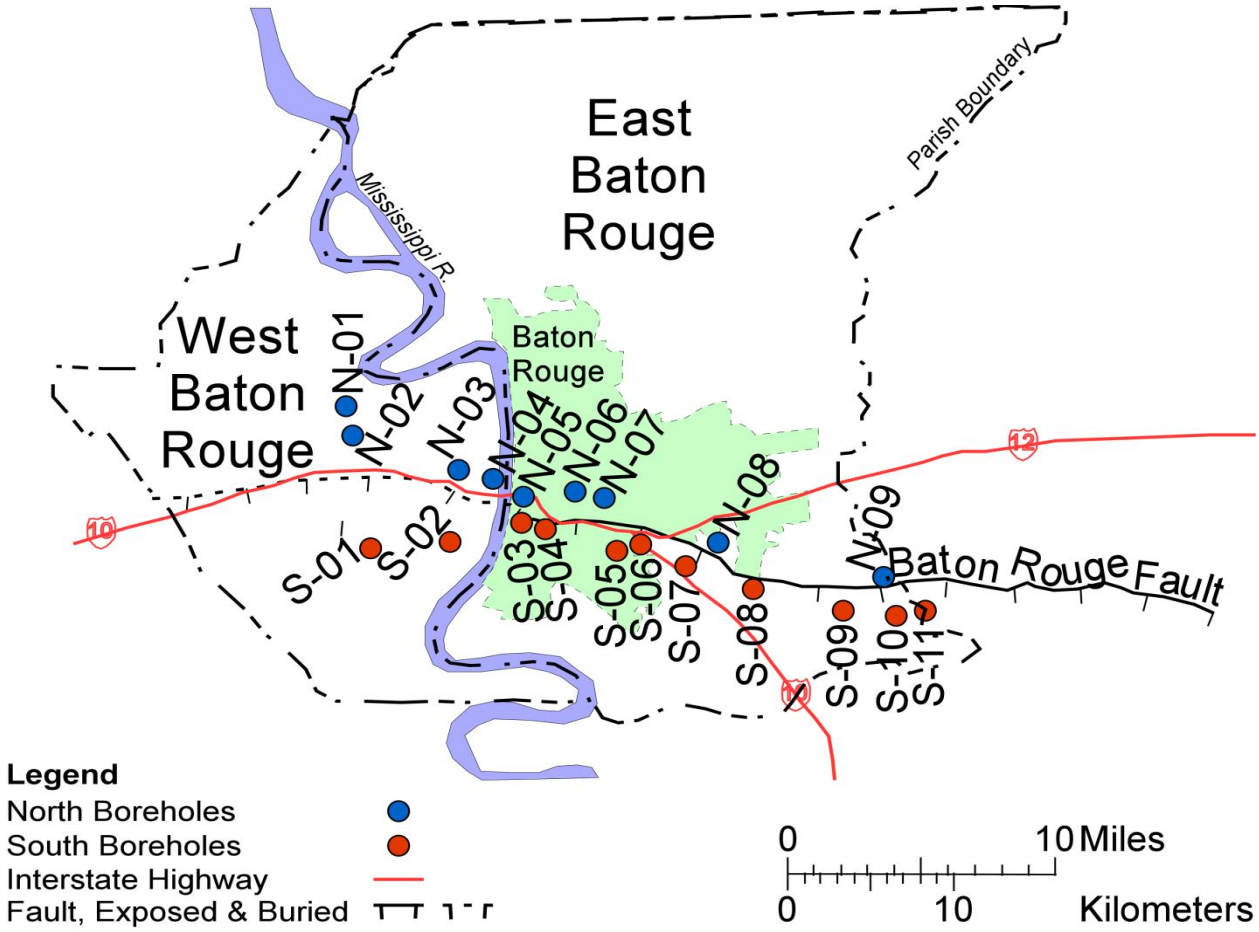

Figure 3.1. Location of nineteen wells comprising two west-east transects, one directly to the north and one directly to the south of the Baton Rouge fault from Wendeborn and Hanor (2008).

Spontaneous potential and resistivity log responses are controlled largely by the ratio of sand to clay minerals and have long been used to interpret environments of sediment deposition, e.g., Kerr and Jirik (1990) and references therein. Galloway (1977) established a meandering stream facies model which recognized channel fill, levee, crevasse splay and floodplain depositional facies (Figure 3.2) Kerr and Jirik (1990) adapted Galloway's (1977) facies model to include well log curve morphologies matching each the fluvial facies (Figure 3.2) based on SP and resistivity responses for known fluvial facies of the middle Frio formation, South Texas. Levee facies result in spiky curve responses. Channel fill pointbar sands are associated with blocky, fining-upwards curve morphology. Crevasse splay deposits have coarsening-upwards

curve morphology and muddy floodplain sediments are associated with baseline SP and resistivity curves. Sands deposited by braided streams produce jagged, wedge-shaped curve morphologies (Figure 3.3, Miall, 2010). The use of these facies models to identify possible fluvial facies based on well log image spontaneous potential is shown in Figure 3.4.

The Frio and Mississippi are similar in that they are both meandering rivers which deposit sediments on an aggrading coastal plain. They differ in terms of scale. The Mississippi River has been identified as one of the world's major river systems on the basis of sediment discharge (Milliman and Meade, 1983) and is a model for a major river dominated delta system (Wright and Coleman, 1973). The Mississippi is thus much larger than the system which deposited the middle Frio formation and the spatial scale of facies presented by Kerr and Jirik (1990) does not apply to the facies of the Mississippi or its ancient analogues.

Spatial scales of depositional elements for the Mississippi and ancient analogues were derived from Figure 2.2. Point bar channel fill sands are about 100 feet thick (Hanor, personal communication) and may extend laterally up to 4 miles (21,120 feet). Natural levee deposits extend between 2.5 and 9 miles (13,200 and 47,520 feet). Crevasse splay deposits are about 1.5 miles (7,920 feet) wide and extend up to 5 miles (26,400 feet). Floodplain facies of the Mississippi River, like those of the Frio formation, have variable dimensions and may be laterally extensive.

Various analytical techniques were applied to well log data for the study area. These included: 1) evaluation of subsurface geology through lithostratigraphic cross sections, 2) resistivity curve shape matching to well log-derived block diagrams and, 3) sequence stratigraphic setting indicated by well log-derived lithology-depth curves.

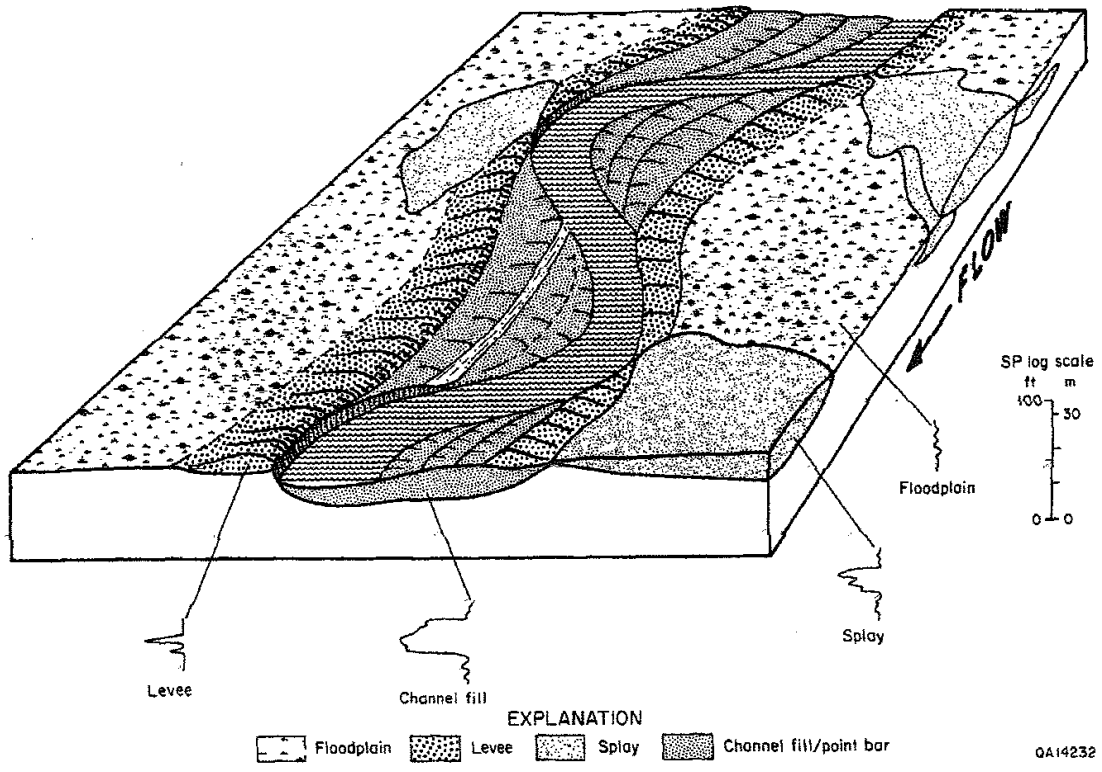

Figure 3.2. A meandering river facies model presented by Galloway (1977) showing floodplain, splay, channel fill, and levee deposits. Kerr and Jirik (1990) provided examples of well log responses that match the fluvial facies based on SP and resistivity data from the Oligocene middle Frio formation, Texas.

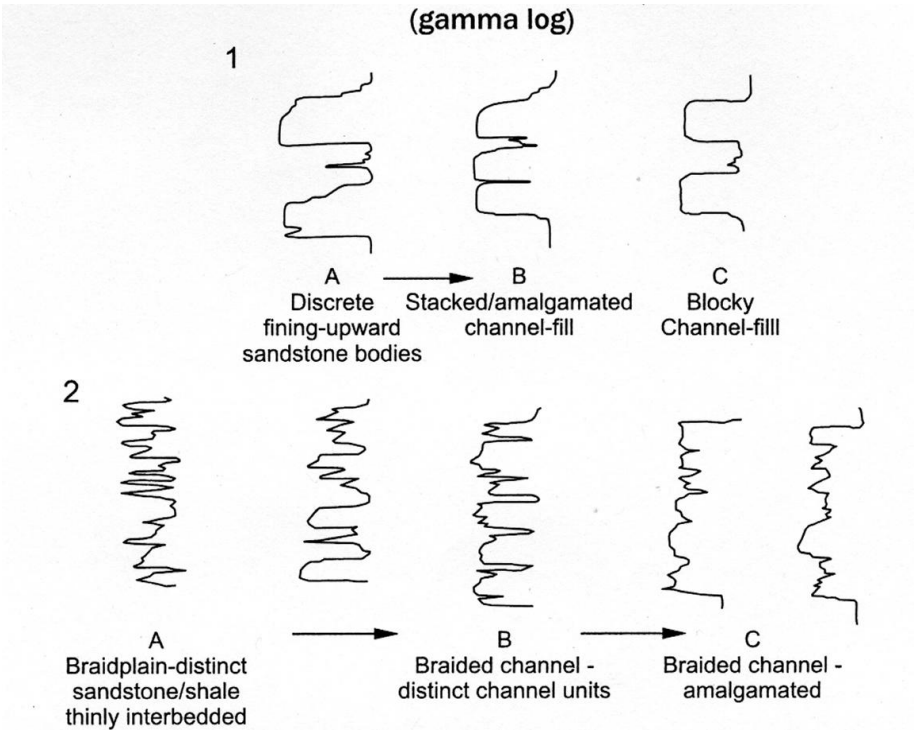

Figure 3.3. Meandering stream channel sands (top) produce blocky, fining upward log responses. Braided stream sands (bottom) produce jagged, wedge-shaped log responses (Miall, 2010).

3.2 Evaluation of subsurface geology through cross sections

Two lithostratigraphic cross sections were drafted along transects established by Wendeborn and Hanor (2008), with one transect directly to the north and one directly south of the Baton Rouge Fault and both running approximately parallel to strike of the aquifer units (Figure 3.1). The north transect (N- transect) included 8 wells with data for the depth interval of 1400 to 2400 feet (425 to 730 m) and the south transect (S- transect) included 11 wells with data from 1400 to 2800 feet (425 to 730 m). Depth intervals correspond to the locations of USGS-identified 1500' to 2400' sands. The additional depth was added to the south transect to include units displaced by the Baton Rouge Fault. SP and resistivity curves for each log were digitized using a program written by Matthew Clark at Louisiana State University, and original log depths were adjusted for Kelley Bushing height and ground level elevation so that the digitized depths

are relative to the National Geodetic Vertical Datum of 1929 (NGVD29). These curves were used to identify the location of sands at depth, with sands identified as deviations from a visually estimated shale or mudstone baseline of both resistivity and SP curves. Figure 3.4 shows a typical log. Boundaries between sands and mudstone were drawn based on points of inflection of the resistivity and SP curve. Sand units were then laterally correlated between logs along each transect. Sands at matching depths for adjacent logs were extended to connect between those logs. Non-sand areas were assumed to be mudstone.

3.3 Isometric fence diagrams and log curve morphologies

Rollo (1969) used isometric fence diagrams to illustrate the geometries of the 1200', 1500', 2000' and 2400' sands. An example is seen in Figure 1.3. Hanor (1971) converted Rollo's (1969) sand figures into block diagrams by covering the fence diagrams with bounding surfaces (Figure 1.4). The Rollo (1969) and Hanor (1971) diagrams neglect the existence of the Denham Springs - Scotlandville fault. There should be some down-to-the-south offset in the northern portions of the diagrams (Tsai, personal communication).

Figures by Hanor (1971) were re-drafted digitally for this study. Boreholes on visible side surfaces of the block diagrams were selected from the original 1969 diagrams to represent a variety of sand unit shapes. Resistivity curves for these logs were drafted and matched to sand units in the 1200', 1500', 2000' and 2400' sand plates shown in the following section. Depositional facies were interpreted for these diagrams using the log response facies model established by Kerr and Jirik (1990) (Figure 3.2).

3.4 Sequence stratigraphic setting using lithology-depth curves

Hanor (personal communication, 2012) used the digital resistivity logs for the transect immediately south of the fault (S-transect) to determine what percentage of all of the logs had a

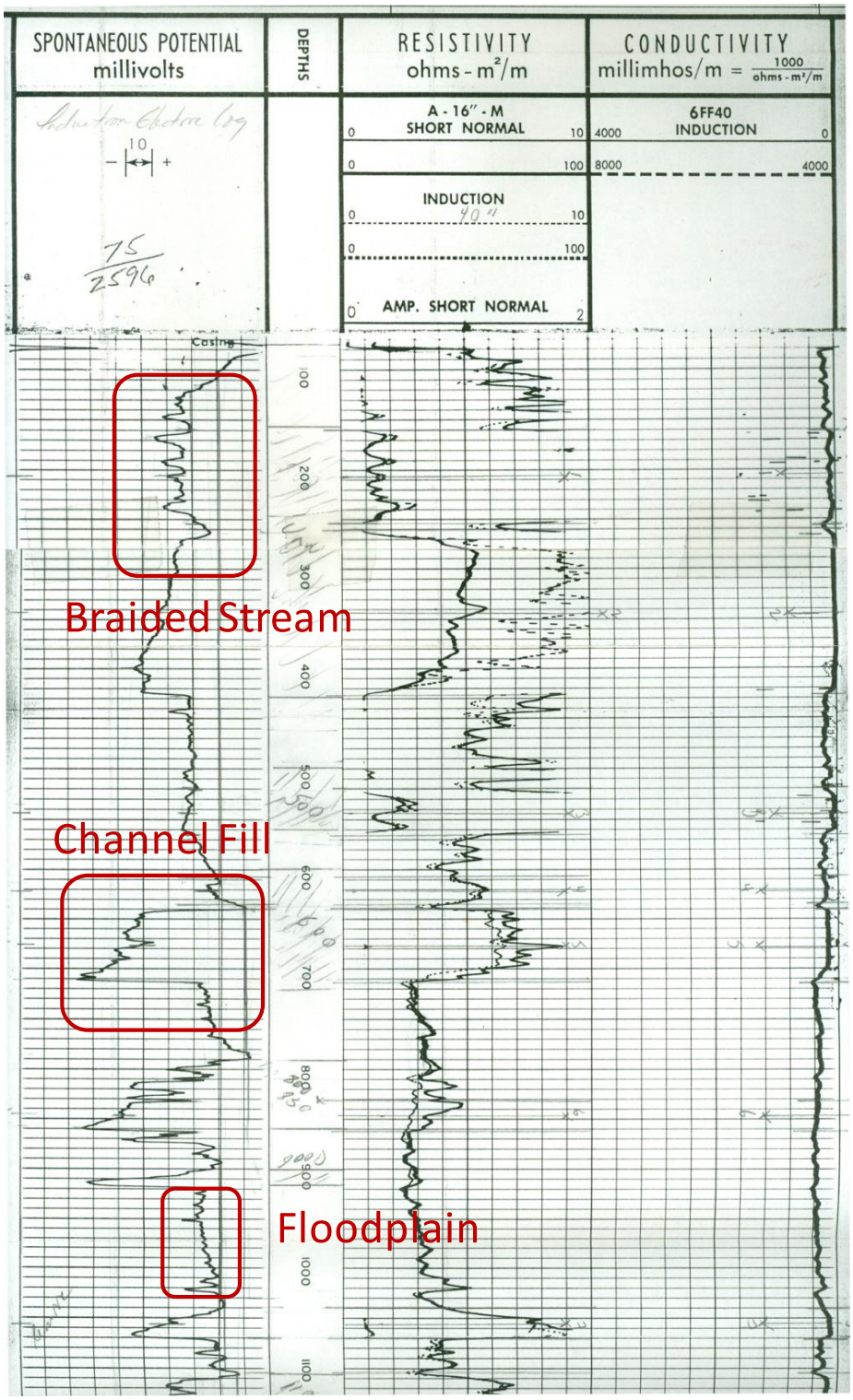

Figure 3.4. A well log interval for borehole S-4 in this study showing representative SP, resistivity and conductivity curves. Possible fluvial facies are identified based on SP curve morphology. Channel fill or pointbar deposits are thick, fining upward sequences. Floodplain facies show a shale baseline SP curve response (Kerr and Jirik, 1990).

resistivity response indicative of mudstone at a specified depth (MSL). This appeared to be a possible way of identifying sand-rich and mudstone-rich stratigraphic intervals in a more quantitative way in a sequence in which individual units are highly discontinuous laterally. For example, if all the logs had a mudstone response, then this depth was assigned a value of 100 for the entire transect. If half the logs had a mudstone response, that depth was assigned a value of 50, and if none did the depth was assigned a value of zero. A plot was then made of mudstone percentage as a function of depth for the entire transect, which proved to be a convenient way of identifying mudstone-rich and sand-rich stratigraphic intervals. The sand-rich intervals appeared to correlate with the USGS "sands". However, these logs used were discretized at one-meter depths (see Appendix A), which limited the resolution of the technique.

To provide a more quantitative analysis of the environments of deposition, five new transects including 50 logs digitized at 0.5-foot intervals were established to the north of N-transect (Figure 1.1). These transects were identified as A-A' through E-E' and run west to east parallel to strike, and perpendicular to the dip of units. The transects run approximately 25 miles (40 km) in length and cover an area of 12 miles (20 km), extending the study area by about an additional 240 square miles (800 km^2) to the north.

Averaged lithology-depth curves were established for the full depth available for each transect based on digital log data. Lithologies for each log were determined from well log long-normal resistivity values for each 0.5 foot interval of each log along a transect. Original log depths were adjusted for Kelley Bushing height and ground level elevation so that the new depths are relative to NAVD29. A cutoff value was assigned based on a visually determined mudstone baseline for each log, which generally fell between 10 and 35 ohm-m. Sediments at depths with a resistivity falling below this baseline were classified as mudstone and assigned a

value of 100, while those above the cutoff were classified as sand and assigned a value 0. These lithologically-qualifying values were then averaged across each transect at a given depth to provide a percent mudstone value for each half foot of depth along the transect. Depths represented with fewer than 6 boreholes were discarded. A 41-point centered moving average was applied because data points were closely spaced. The percent mudstone was graphed as a function of depth and trends were correlated between transects. Curves were drawn for the S- and N- transects following methods established by Hanor (personal communication, 2012) but were not used here because of the short depth interval of the logs and the one-meter depth spacing of the data points.

4. RESULTS

4.1 Evaluation of subsurface geology through cross sections

Figures 4.1 and 4.2 show SP and resistivity curves for the west-east cross sections immediately north and south of the fault, and inferred location and extent of sand bodies and confining mudstones. Both transects reveal a high volume of mudstones and laterally discontinuous sands. USGS-identified aquifer units such as the 2000' sand are clearly not continuous laterally across this section. Sand body morphology is highly heterogeneous and includes blocky thick sands, thin laterally extensive sands and isolated sand lenses. These are interbedded with confining mudstones. Examples of log curve morphology representative of different fluvial facies are shown in Figure 4.3.

4.2 Isometric fence diagrams and log curve morphologies

Figures 4.4 and 4.5 show three dimensional sand morphologies in aquifer units adapted from Rollo (1969) and Hanor (1971). Sand plates for the 1200', 1500', 2000' and 2400' sands are shown with expanded spacing in Figure 4.4 to allow each sand unit to be viewed individually, while Figure 4.5 has a tighter spacing of sand plates intended to more realistically show the subsurface. Resistivity curves for selected logs are shown for the 1200', 1500', 2000' and 2400' sand plates in Figures 4.6, 4.7, 4.8 and 4.9.

Many of the sands appear to be channel fill sands (point bar sands). This is evident in the 1200' sand, where the selected log responses are largely indicative of blocky, upwardly fining units (Figure 4.6). Further log analysis indicates stacking of multiple sand units to comprise layers depicted as homogeneous by Rollo. A clear example is the 400-foot interval of stacked sands at Li-56 in the 2000' sand diagram (Figure 4.8).

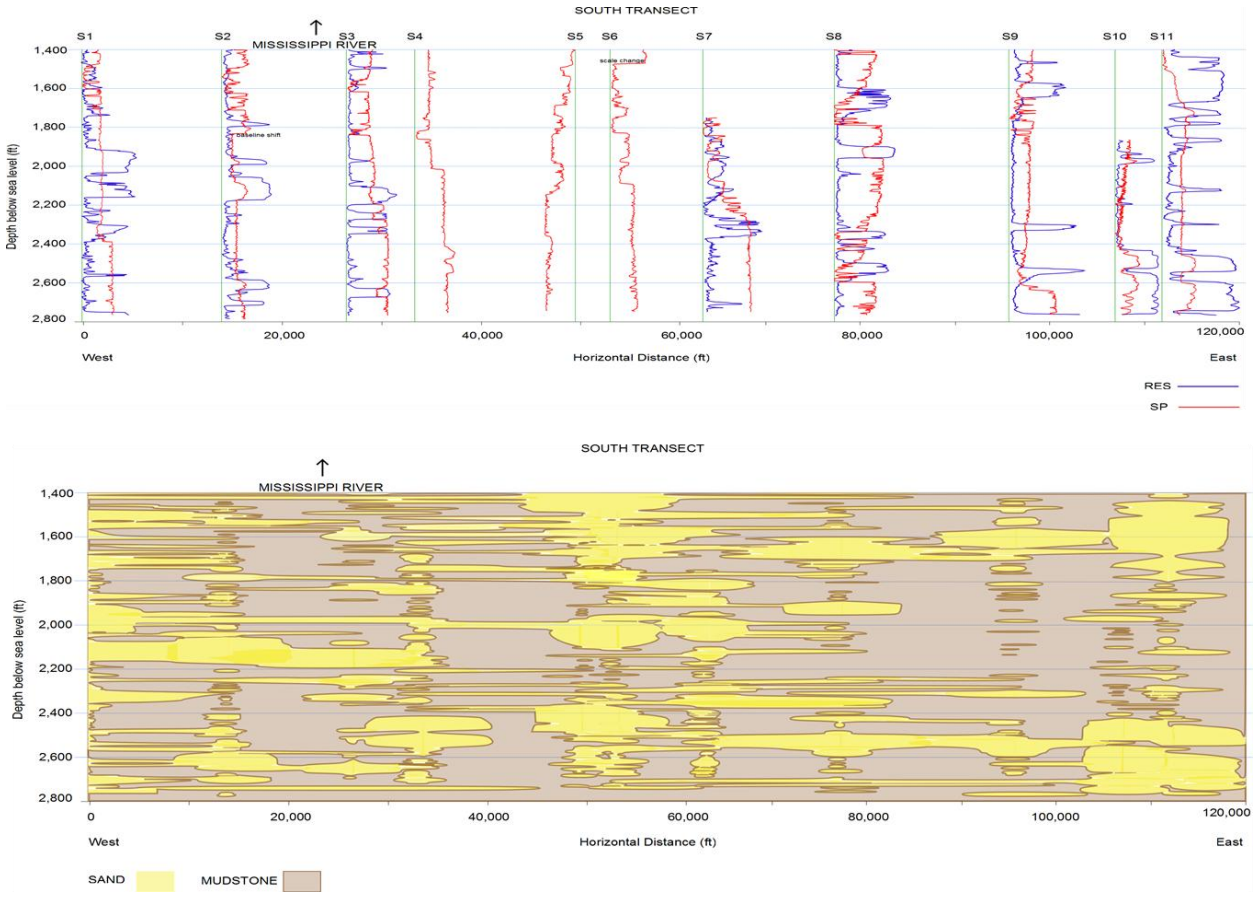

Figure 4.1. South (S-) transect. Spatial distribution of sands and mudstones and their lateral correlation (bottom) were drafted from SP and resistivity responses (top) for 11 wells south of the Baton Rouge fault and included the depth interval of 1,400 to 2,800 feet.

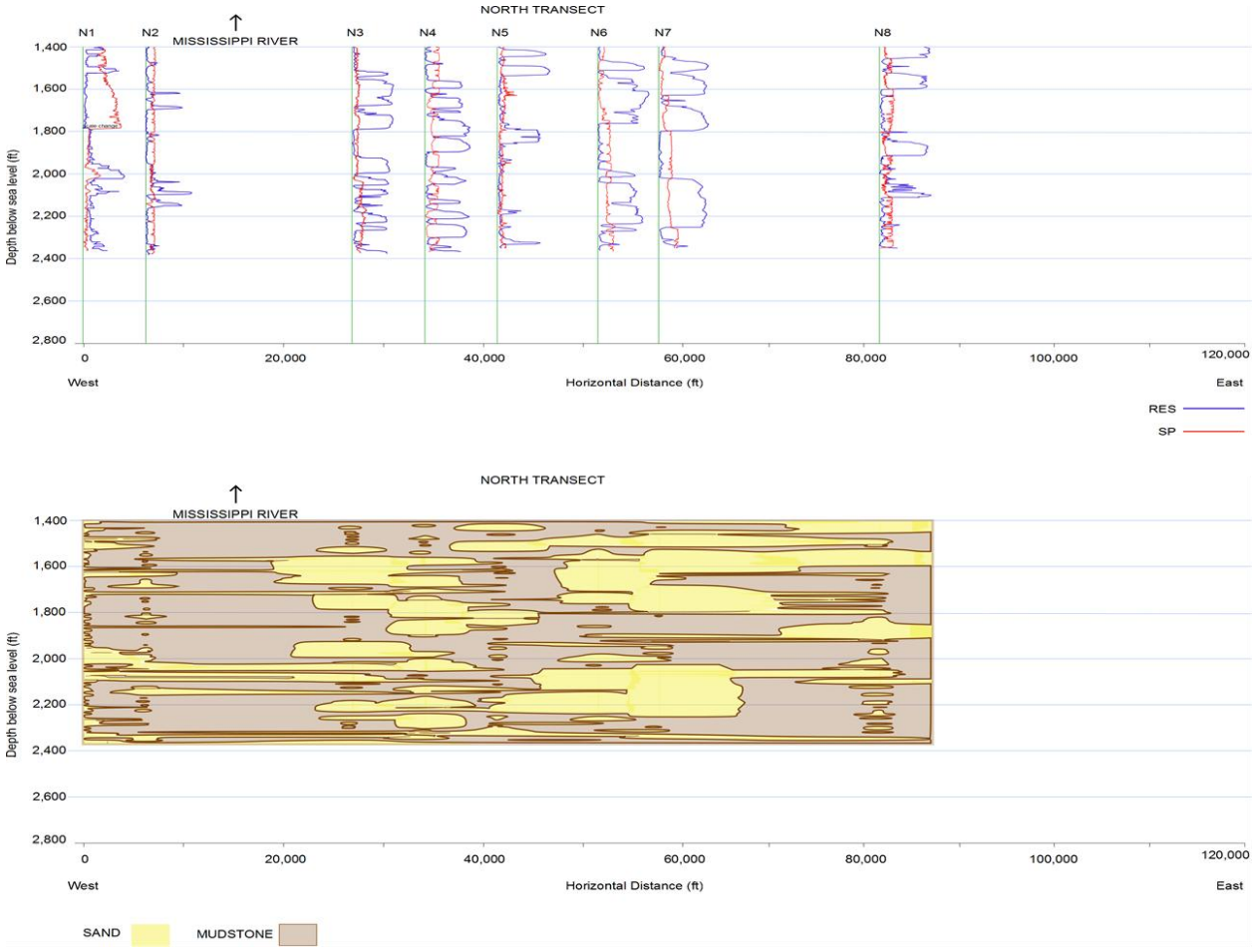

Figure 4.2. The north (N-) transect included SP and resistivity data (top) and the correlation of sands and mudstones (bottom) for the depth interval of 1,400 to 2,400 feet from 8 wells directly to the north of the Baton Rouge fault.

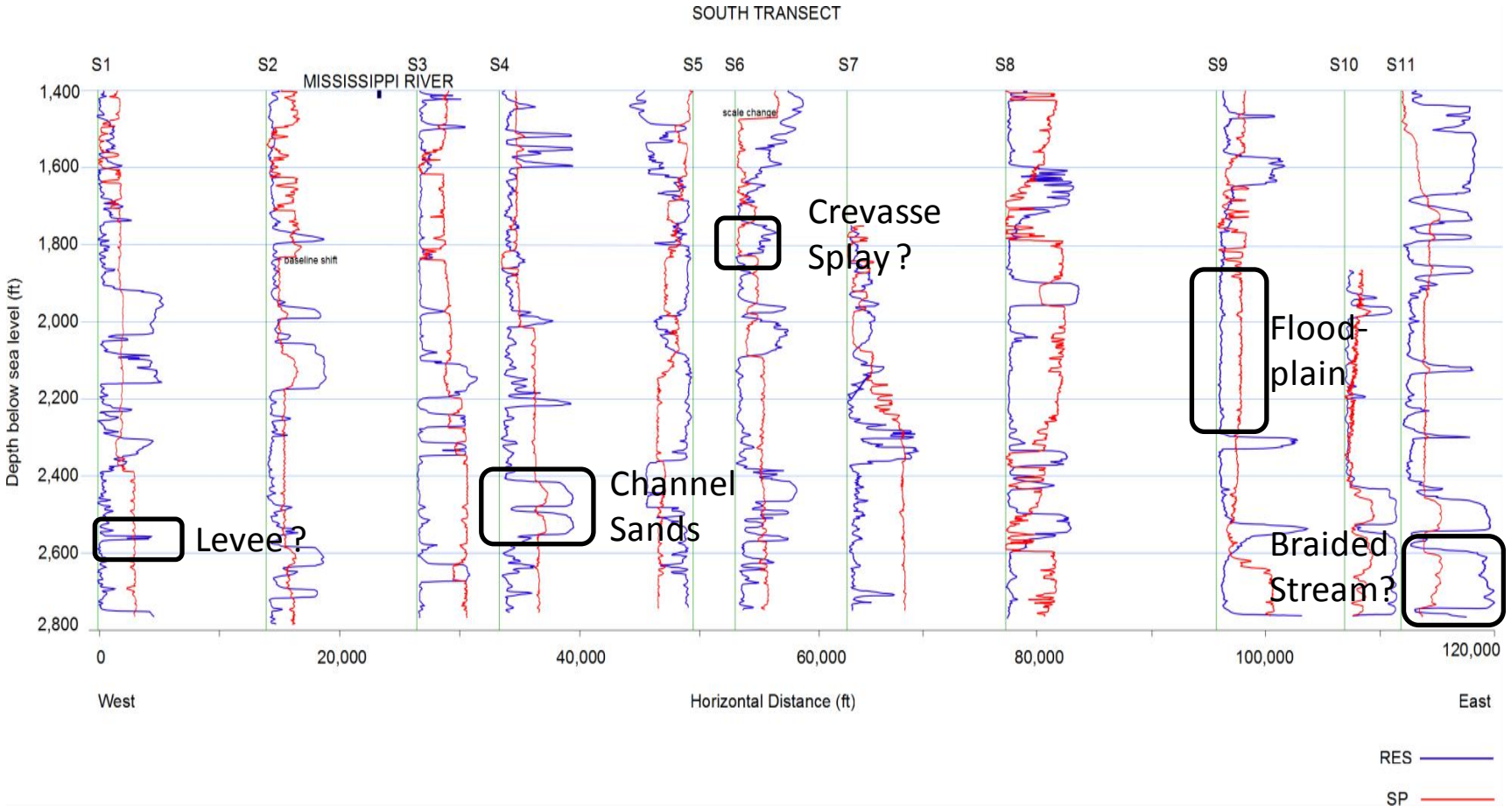

Figure 4.3. Examples of possible fluvial facies identified in resistivity and SP log responses for the south transect.

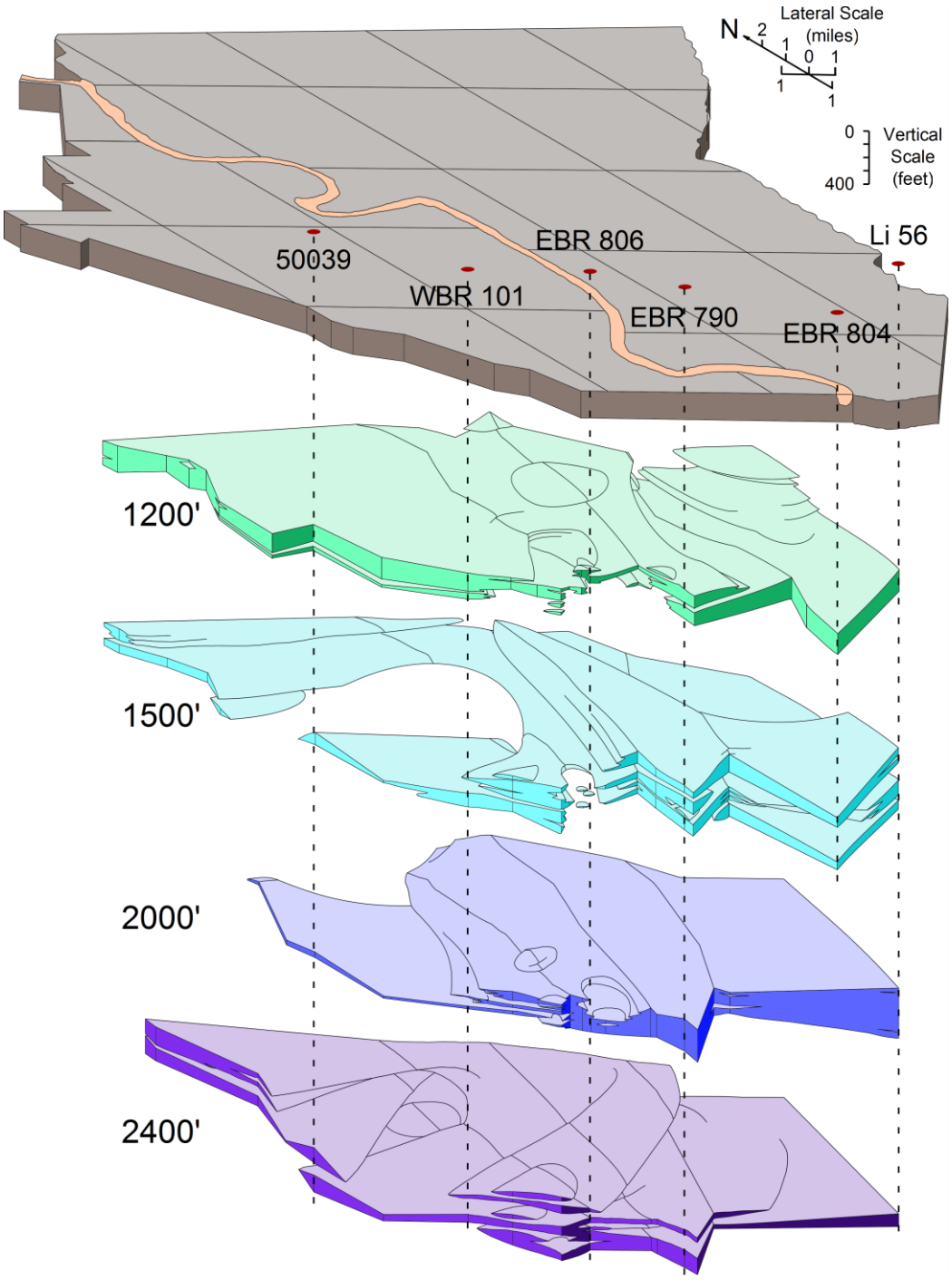

Figure 4.4. Expanded spacing of the 1200', 1500', 2000' and 2400' sands, adapted from Hanor (1971) and Rollo (1969). 50039, WBR 101, EBR 806, EBR 790, EBR 804 and LI 56 are boreholes used for matching curve morphologies.

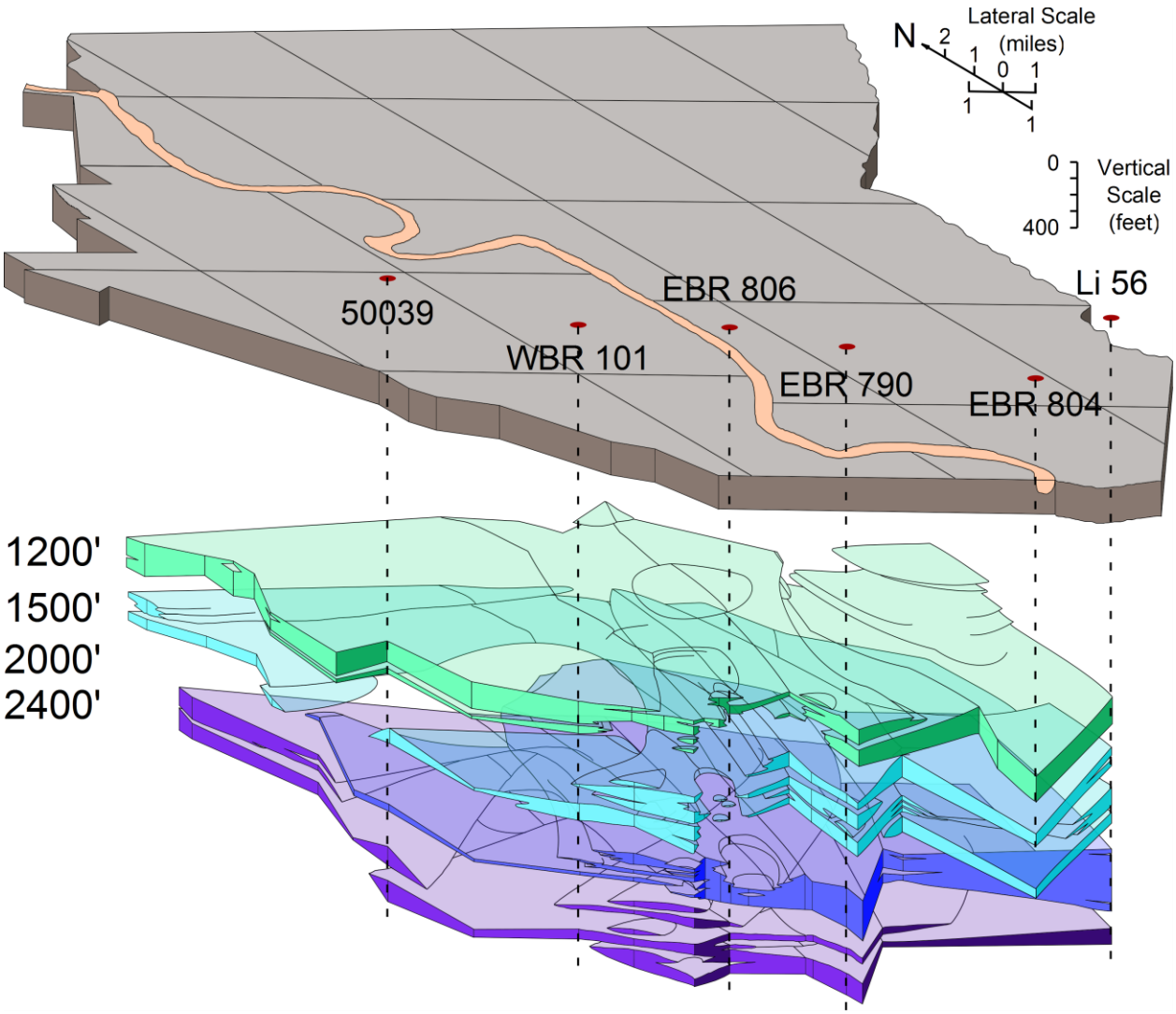

Figure 4.5. Actual scaled vertical spacing of the 1200', 1500', 2000' and 2400' sand units adapted from Hanor (1971) and Rollo (1969).

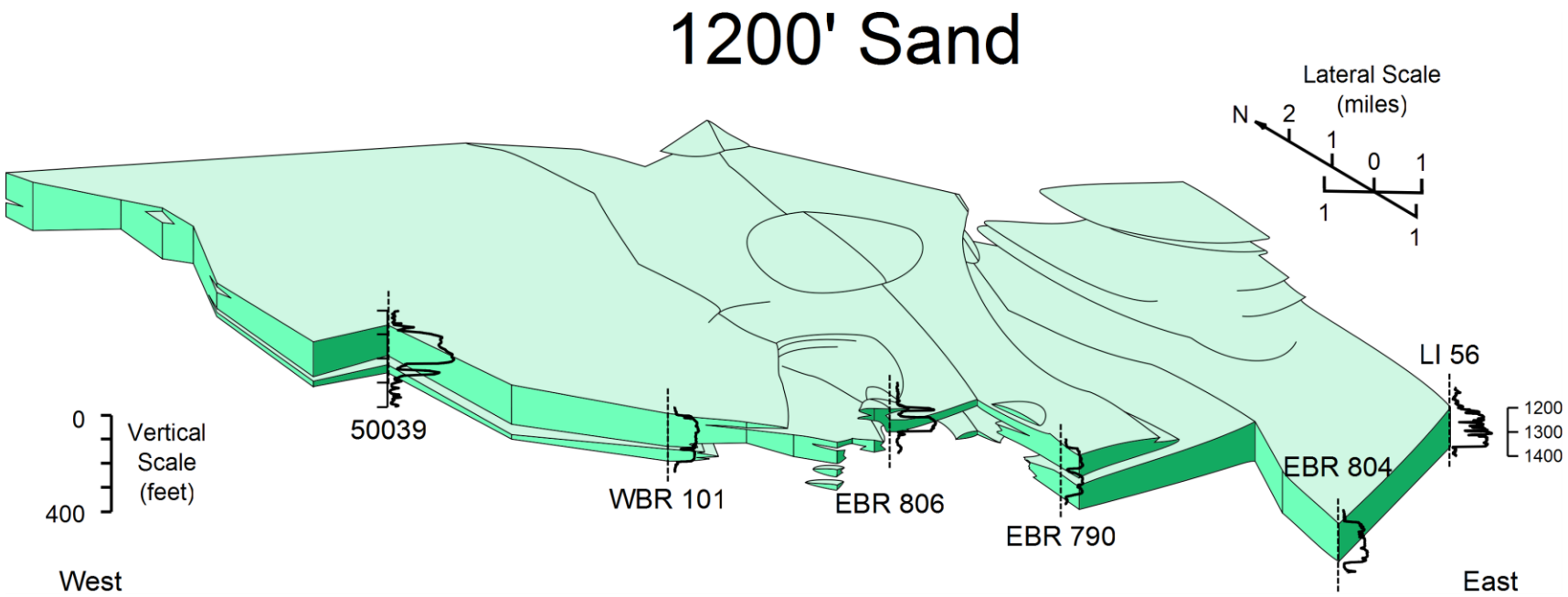

Figure 4.6. Block diagram of the 1200' sand (Hanor, 1971) with resistivity curves added for selected wells. Amalgamated sands are seen at LI 56. The curve morphologies at EBR 790 suggest channel fill and levee facies. The vertical scale on the right shows depth relative to mean sea level.

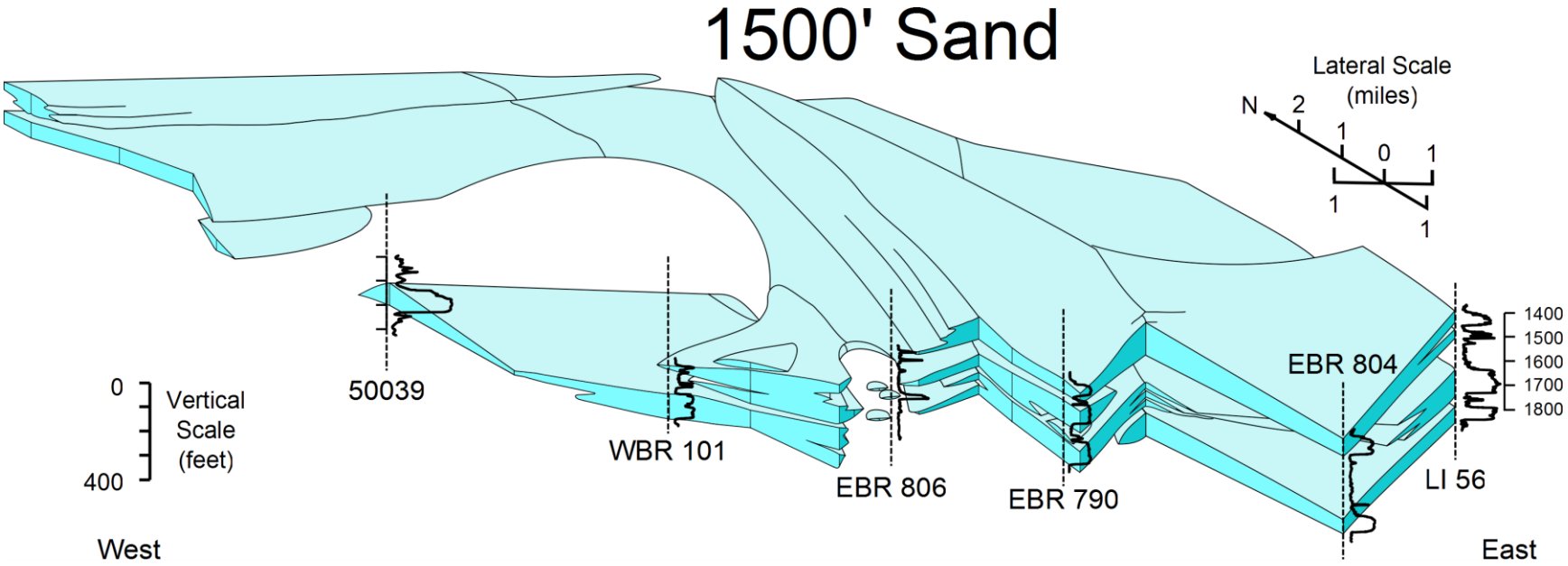

Figure 4.7. Block diagram of the 1500' sand (Hanor, 1971) with resistivity curves added for selected wells. The curve for sands at borehole 50039 is exemplary of the blocky, fining-upwards morphology associated with channel fill facies. EBR 804 has two sand units separated by an area with baseline resistivity response which indicates a floodplain facies. There are three isolated sand lenses near EBR 806. The vertical scale on the right shows depth relative to mean sea level.

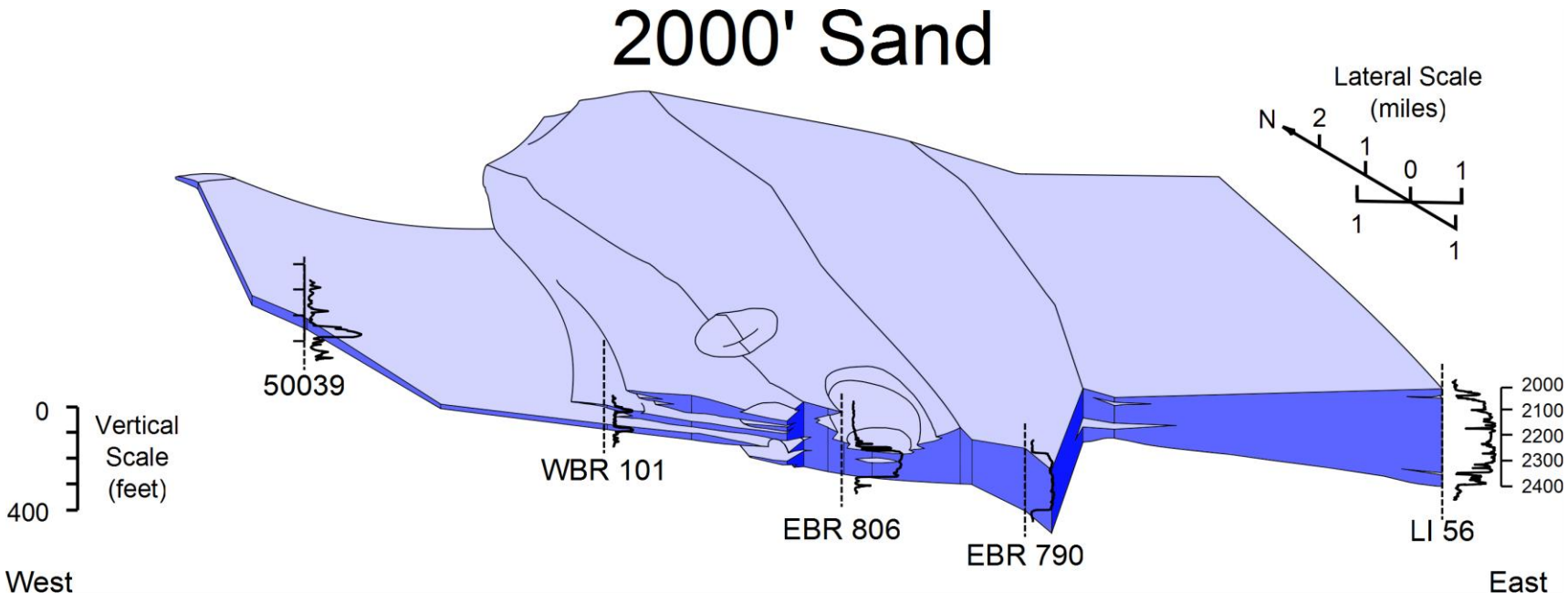

Figure 4.8. Block diagram of the 2000' sand (Hanor, 1971) with resistivity curves added for selected wells. Amalgamated sands are seen at LI 56. Sands thin and pinch out to the west which suggests an erosional unconformity. The vertical scale on the right shows depth relative to mean sea level.

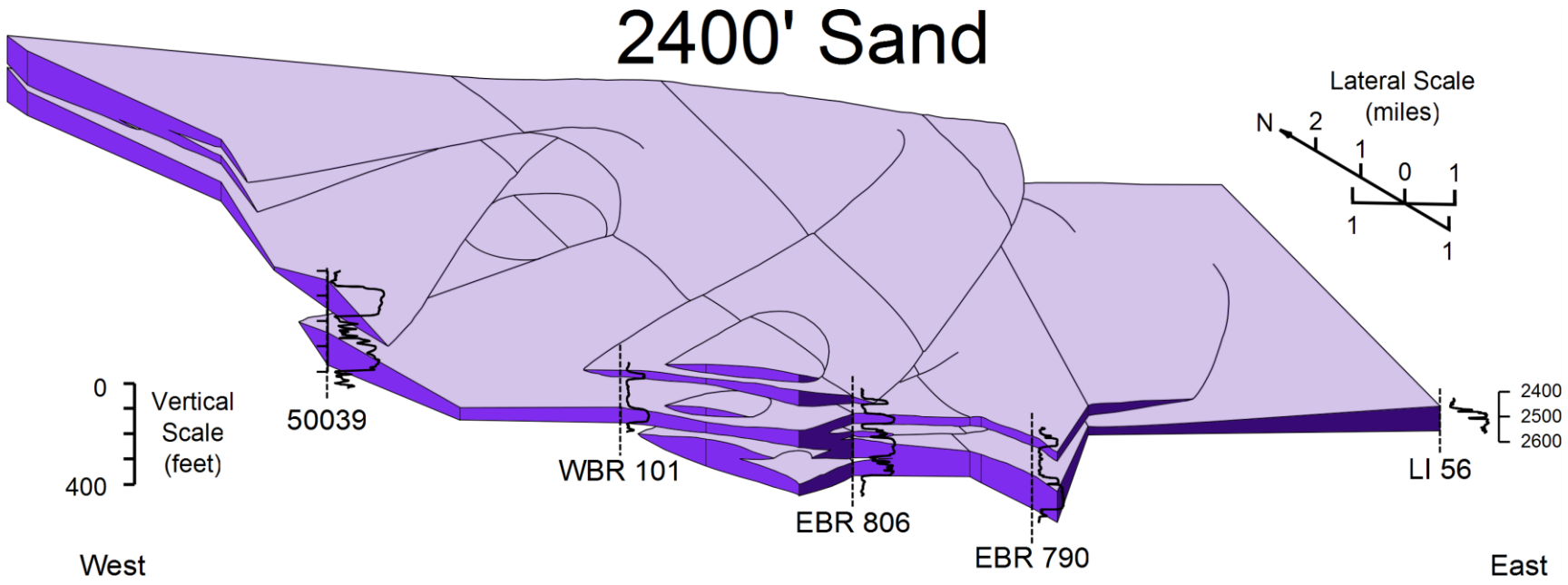

Figure 4.9. Block diagram of the 1500’ sand (Hanor, 1971) with resistivity curves added for selected wells. A channel fill facies curve morphology is present at WBR 101. The vertical scale on the right shows depth relative to mean sea level.

4.3 Sequence stratigraphic setting using lithology-depth curves

Plotting average percent mudstone with depth for each transect yielded five curves showing changes in average lithology with depth and position down-dip within the study area (Figure 4.10). These curves reveal cyclic peaks with depth. Each peak to the left in Figure 4.10 represents a high percentage of sand across the transect at that depth, while far-right portions of the curve indicate high average percent mudstone across that transect at the given depths. Sand-rich zones established in this study (Figure 4.11) were correlated with the USGS-designated sand units based on zones established in Griffith's (2003) cross section through the study area (Figure 1.2). The sand peaks were also correlated from one transect to another. For example, the 1200' sand exists as a strong peak in all transects and occurs at increasing depths from northernmost transect A-A' to southernmost transect E-E' (Figure 4.10). The dip of the sand maximum in for the 1200' sand in these curves is 0.429 degrees south and the offset on the Denham Springs-Scotlandville fault is 75.3 feet (Hanor, personal communication). Enlarged curves with labeled sand units for transects A-A', B-B', C-C' and D-D' are shown in Appendix B.

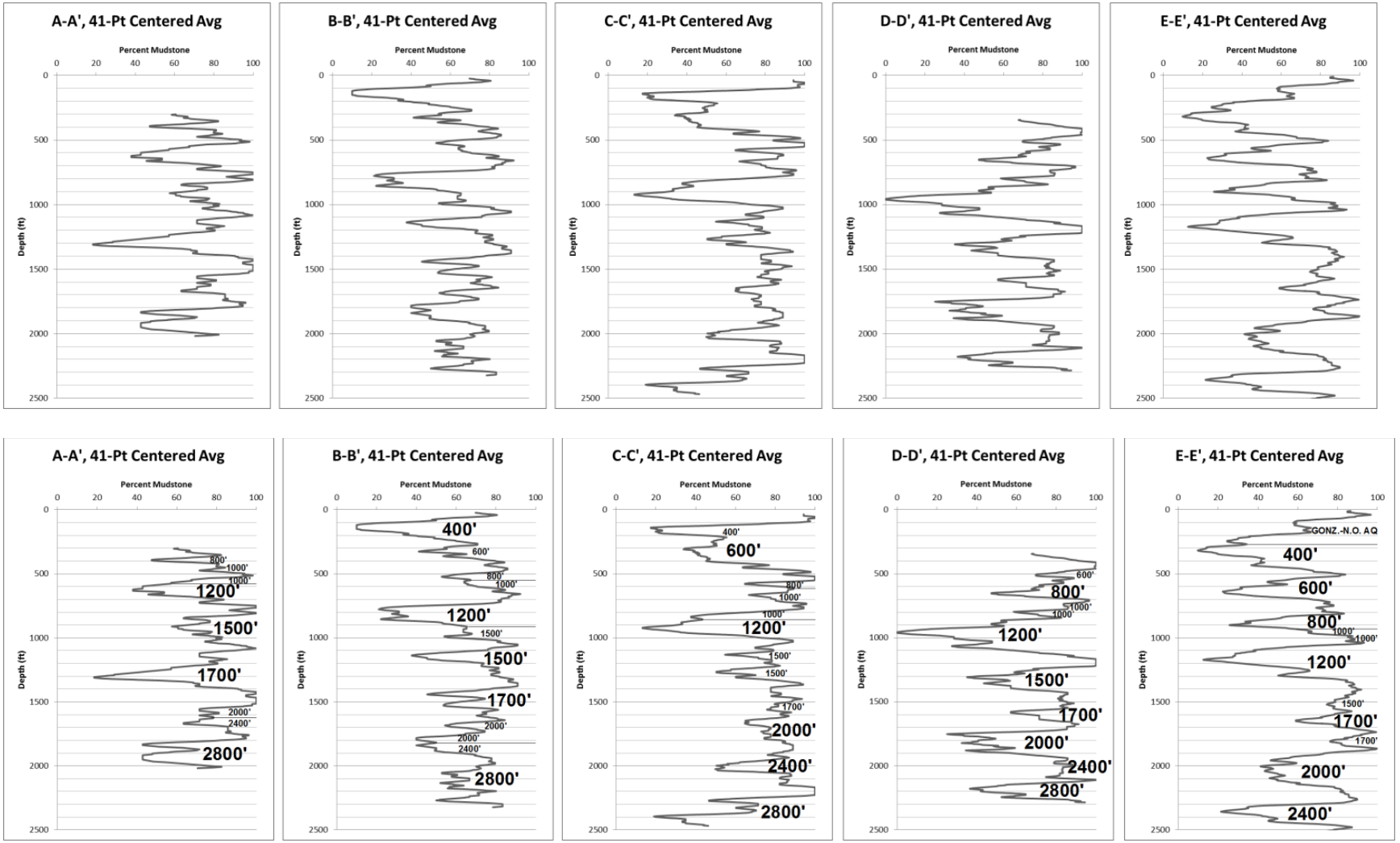

Figure 4.10. Averaged lithology-depth curves for transects A-A' through E-E' (top). The scale 0 to 100 at the top of each graph represents the percentage of the logs in that transect which have mudstone present at that given depth. A 41-point centered average was used to smooth the data. Peaks to the left thus indicate a high proportion of sand across the transect, while peaks to the right indicate a high proportion of mudstone. Sandy peaks are labeled to corresponding USGS-designated sands (bottom).

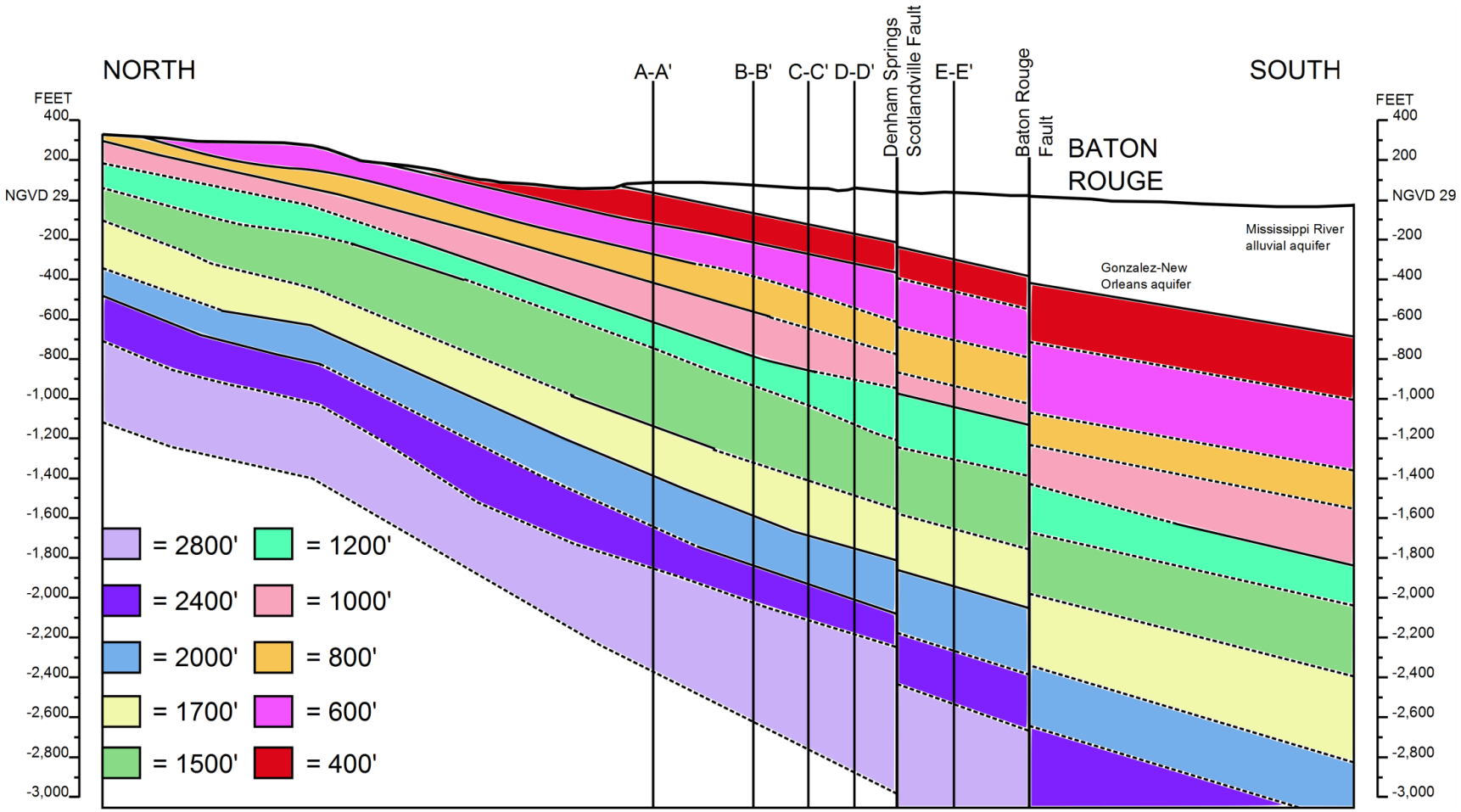

Figure 4.11. Depth zones in which USGS-designated sand units occur, adapted from Griffith (2003). Note the offset of units due to the Denham Springs-Scotlandville and Baton Rouge faults.

5. DISCUSSION

5.1 Baton Rouge aquifer stratigraphy

The isometric fence diagrams of sand units were useful in guiding interpretations of Baton Rouge Aquifer stratigraphy, particularly of the 1500', 1700' and 2000' sands. As shown in Figure 4.4, the 2000' sand pinches out to the west. Above it, the 1500' sand thins and shows channel body fill log morphology at log 50039. The westward absence of the 2000' sand may be due to removal of sediment by incision of an overlying channel which deposited the 1500' sand at that location. This is similar to an unconformity documented by Griffith (2003) to the east of the study area, where the 1500' and 1700' sands merge to form the Kentwood Aquifer. The 1500' sand appears to cut into the 1700' sand at this location. The Mississippi River Alluvial Aquifer overlies Pleistocene terraces to the west of the study area and is another known example of a major unconformity.

Sands occurring within the USGS-designated 1700' sand depth are included in Rollo's (1969) 1500' sand diagram (Figure 1.3). Small sand islands identified at EBR-806 in the 1500' sand are likely channel bodies deposited by relatively small second to third order streams (Figure 4.7). It is notable that the log curve matches the fining-upward morphology identified by Kerr and Jirik (1990) for channel body fill fluvial facies. However, the small size of this sand unit could easily lead to misidentification as an isolated sand peak in a levee facies, illustrating the ambiguity of log curve-facies identification in a single log.

Lithology-depth curves for the 1500' and 1700' sands show strong peaks in all transects except C-C' and are frequently separated by a jagged small peak for which the USGS sand correlation remains unclear (Figure 4.10). The ambiguity of the division for these peaks may have led to Rollo's (1969) inclusion of the 1700' sand in the 1500' sand diagram. The separating

peaks may represent a discrete depositional event or events. Sediments deposited during this event could act as a separate aquifer unit, but are not currently recognized as such.

Overall, the lithology-depth curves correlate with the USGS-designation of aquifer sands. Alternating high-sand versus high-clay concentration units seen in Figure 4.10 agree with the number and depth of aquifer sands recognized by the USGS. These peaks occur at incrementally increasing depths from north to south consistent with the dip of the aquifer units toward the Gulf of Mexico. Transect E-E' (Figure 5.1) best matches the USGS-designated aquifer units due to its proximity to the sand unit naming area in north Baton Rouge. Section E-E' is thus taken as the type section for this study.

5.2 Baton Rouge aquifer sand morphologies

Fluvially deposited sediments are sensitive to spatial variations governing sediment transport properties within the river system which result in the deposition of different facies (Miall, 2010). A natural fluvial system deposits genetic sequences of facies ranging from thick sandy channel forms, extensive sandy crevasse splays, finely interbedded levee sands and clays to muddy floodplains (Galloway, 1977; Kerr and Jirik, 1990). The presence of the modern Mississippi River and assumption of the existence of an ancient analogue suggest that Miocene to Pleistocene sediments in the study area were fluvially deposited. This is supported by the location of Miocene to Pleistocene deltas south of the study area (Galloway, 2001) (Figure 2.1) which would have been fed by major river systems and by sand body morphologies identified in the N- and S- cross sections and isometric diagrams.

The N- and S- cross sections Figures 4.1 and 4.2) and block diagrams (Figures 4.4, 4.5, 4.6, 4.7, 4.8 and 4.9) reveal a highly variable and heterogeneous subsurface of interconnected, morphologically complex sands and confining clays. Sands across the entire transect appear

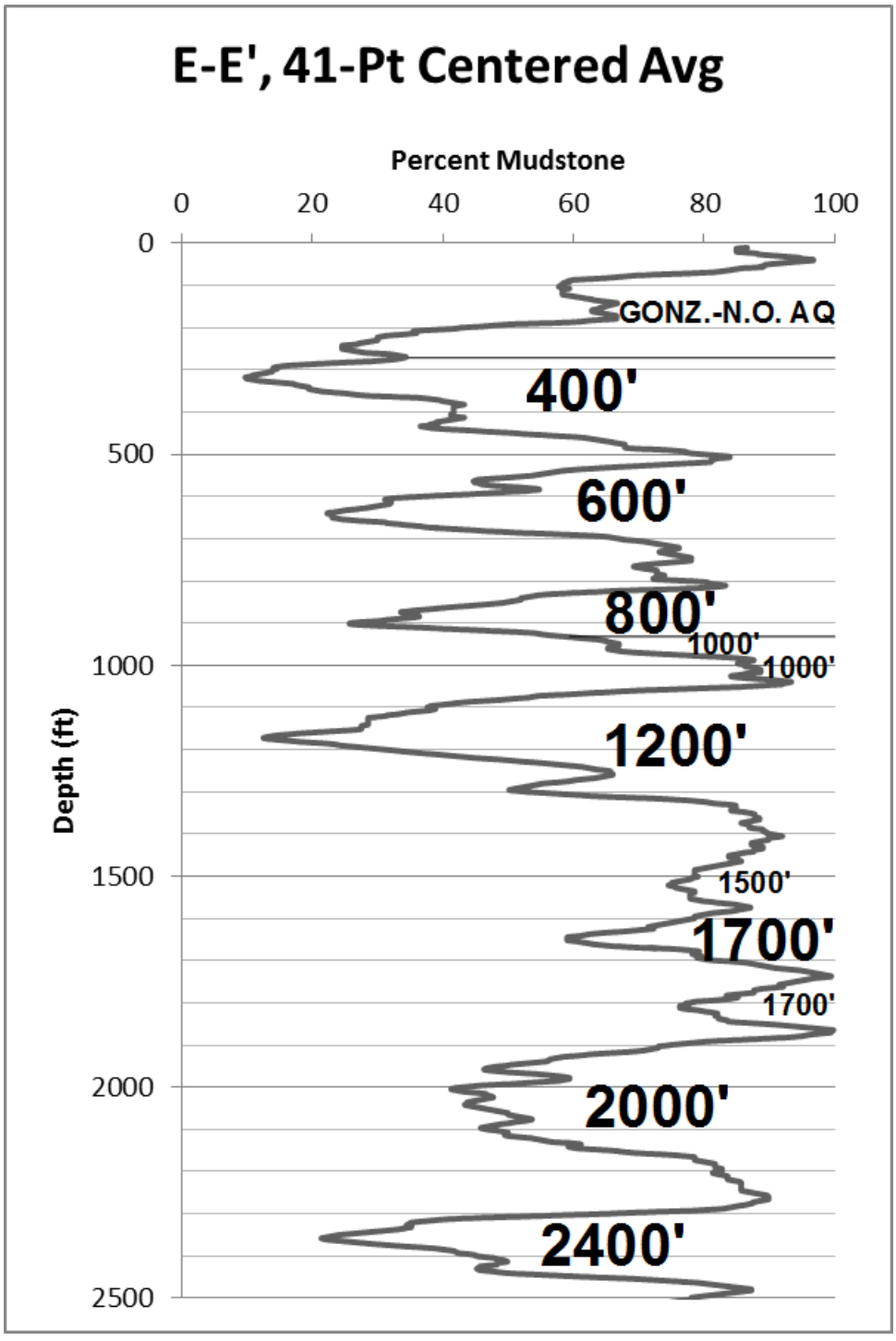

Figure 5.1. The lithology-depth curve for transect E-E' best matches the USGS-designated aquifer units due to its proximity to the sand unit naming area in north Baton Rouge. Section E-E' is thus taken as the type section for this study. Aquifer sands were deposited during times of low aggradation. Mudstone-rich sequences that separate these sandy zones were deposited during times of high aggradation.

discontinuous in two dimensions, and yet are known to behave at specific depths as discrete aquifer units, suggesting hydraulic continuity in three dimensions. The complex morphology and amalgamation of sand bodies is interpreted here to be the result of overlapping and stacked genetic sequences of fluvial facies.

An example of large channel sands is seen in the 2,000 to 2,200 foot depth interval in the west side of the S- cross section, below the location of the modern Mississippi River (Figure 4.1). These sands extend up to 35,000 feet laterally and are approximately 100 feet thick and are therefore comparable in terms of thickness, but appear to be more laterally extensive, than the point bar facies of the modern Mississippi River identified in Figure 2.2. The agreement in thickness suggests deposition by a similarly large river system. The lateral extent of these channel sands indicates possible contemporaneous deposition and movement of the channel from east to west. It could also represent multiple discrete channel body forms connected by sequences of erosion and deposition. This difference may also simply be due to the angle at which the cross section intercepted the sands. Potential differences between the scale sand bodies identified in this work and those deposited by the modern Mississippi River are attributed to variation in sizes and fluvial style (i.e. meandering river, braided stream) of paleochannels which deposited Baton Rouge aquifer sediments.

The high degree of complexity inferred from well-log interpretation of these buried Miocene to Pleistocene sediments is realistic. It is consistent with variations in contemporaneously deposited fluvial units seen in Galloway's (1977) fluvial facies diagrams and with documented geomorphology of present-day systems. The modern Mississippi River is a highly complex fluvial system (Figure 2.2) and it may be an analogue for the older systems that deposited the some of the sands comprising Baton Rouge aquifer units.

The lateral extent of sands in the N- and S- cross sections is based on curve magnitude and horizontal correlation of peaks between logs. This approach introduced error in estimating overall sand within the system. The lateral extent of sand bodies on the hand-drafted cross sections may be too high, while small sand bodies located between mapped logs may be underrepresented due to a lack of data between logs. Mathematical models might reduce this error through a stochastic approach (Tsai, 2010).

5.3 Potential forcing agents

Allogenic (external) and autogenic (intrinsic) controls are forcing agents that act on river systems (Miall, 2010). These controls are important in understanding the depositional environments of Baton Rouge aquifer sediments because they influence fluvial processes governing sediment deposition and preservation. It was hypothesized that the cyclic deposition of sand-rich and clay-rich intervals evident in the lithology-depth curves generated in this study could be linked to the action of forcing agents on the fluvial systems that deposited the Baton Rouge aquifer system. Sea-level change and channel avulsion are possible forcing agents which caused differences in sand versus mudstone content with depth in the study area. Timescales of processes were used in this study to identify the most likely source of sand versus mudstone cyclicity in averaged lithology-depth curves for transects A-A' through E-E'.

Channel avulsion occurs when the river channel breaks out of its natural levee and may create a new river channel or a crevasse splay, and is an example of an autogenic control on fluvial deposition (Miall, 2010). Avulsion is a natural process which favors more hydraulically efficient pathways (Roberts, 1997). Sea-level change is a downstream control that acts on fluvial systems and is an example of an allogenic forcing agent (Blum and Törnqvist, 2000). Miall (2010) indicated that sea-level (Groups 8, 9 and 10 in Table 5.1) is a forcing agent which acts on

a timescale of 10^4 to 10^7 years (Table 5.1). Channel avulsions (Group 7) act on timescales of 10^3-10^4 years (Miall, 2010).

The sediments of the Baton Rouge Aquifer System were deposited over a period of about 7 to 10 million years, from the upper Miocene through the Pleistocene (Table 2.1). Roughly 10 distinct sand peaks are identified in lithology-depth curves for these sediments (Figure 4.10). The relatively short timescale on which avulsions occur was deemed unlikely to cause patterns showing 10 cycles in a ten million year period, even with a high occurrence of unconformities. Therefore, we can reject channel avulsion as a forcing agent for the cyclicity evident in the lithology-depth curves generated in this study. Further investigation in this study focused on the effects of sea-level change on lithology and preservation in the rock record.

5.4 The influence of sea-level change on lithology

Changes in sea-level affect lithology by influencing the processes that govern sediment deposition (Posamentier and Allen, 1999). During sea-level falling-stage and lowstand system tracts, river slope is increased and valley incision occurs. This is associated with degradation and the production of erosional unconformities, which are then overlain by sand bodies. As sea-level rises, aggradation rate increases (Figure 5.2).

These changes in aggradation rate are reflected in the preserved lithostratigraphy. The removal of muds during times of low aggradation rate leads to the preservation of units with high sand concentrations and amalgamated sand geometries (Figure 5.3). Higher preservation of muddy units deposited during periods of high aggradation results in a lower concentration of sands that are more highly compartmentalized (Kerr and Jirik, 1990).

The result is a depositional sequence bounded by erosional unconformities overlain with amalgamated sands (Posamentier and Allen, 1999). Rises in sea-level are associated with the

Table 5.1. Miall's (2010) hierarchy of alluvial depositional units and time scales. Milankovitch cycles included in groups 8, 9 and 10 may cause sea-level change (Miall, 2010).

Group	Time scale of processes (yrs.)	Examples of processes	Fluvial, Deltaic depositional units	Rank and characteristics of bounding surfaces
1	10^{-6}	burst-sweep cycle	lamina	0^{th}-order, lamination surface
2	10^{-5}-10^{-4}	bedform migration	ripple (microform)	1^{st}-order, set bounding surface
3	10^{-3}	bedform migration	diurnal/seasonal dune increment, reactivation surface	1^{st}-order, set bounding surface
4	10^{-2}-10^{-1}	bedform migration	dune (mesoform)	2^{nd}-order, co-set bounding surface
5	100-10^{1}	seasonal event, 10-year flood	macroform growth increment	3^{rd}-order, dipping 5-20^{o} in direction of accretion
6	10^{2}-10^{3}	100-year flood, channel and bar migration	macroform (point bar, levee, splay), immature paleosol	4^{th}-order, convex-up macroform top, minor channel scour, flat surface bounding floodplain element
7	10^{3}-10^{4}	long term geomorphic (channel avulsion)	channel, delta lobe, mature paleosol	5^{th}-order, flat to concave-up major channel base
8	10^{4}-10^{5}	5^{th}-order Milankovitch cycles, or response to fault pulse	channel belt, alluvial fan, minor sequence	6^{th}-order, sequence boundary; flat, regionally extensive or base of incised valley
9	10^{5}-10^{6}	4^{th}-order Milankovitch cycles, or response to fault pulse	major depositional system, fan tract, sequence	7^{th}-order, sequence boundary; flat, regionally extensive or base of incised valley
10	10^{6}-10^{7}	3^{rd}-order Milankovitch cycles, tectonic and eustatic processes	basin-fill complex	8^{th}-order, regional disconformity

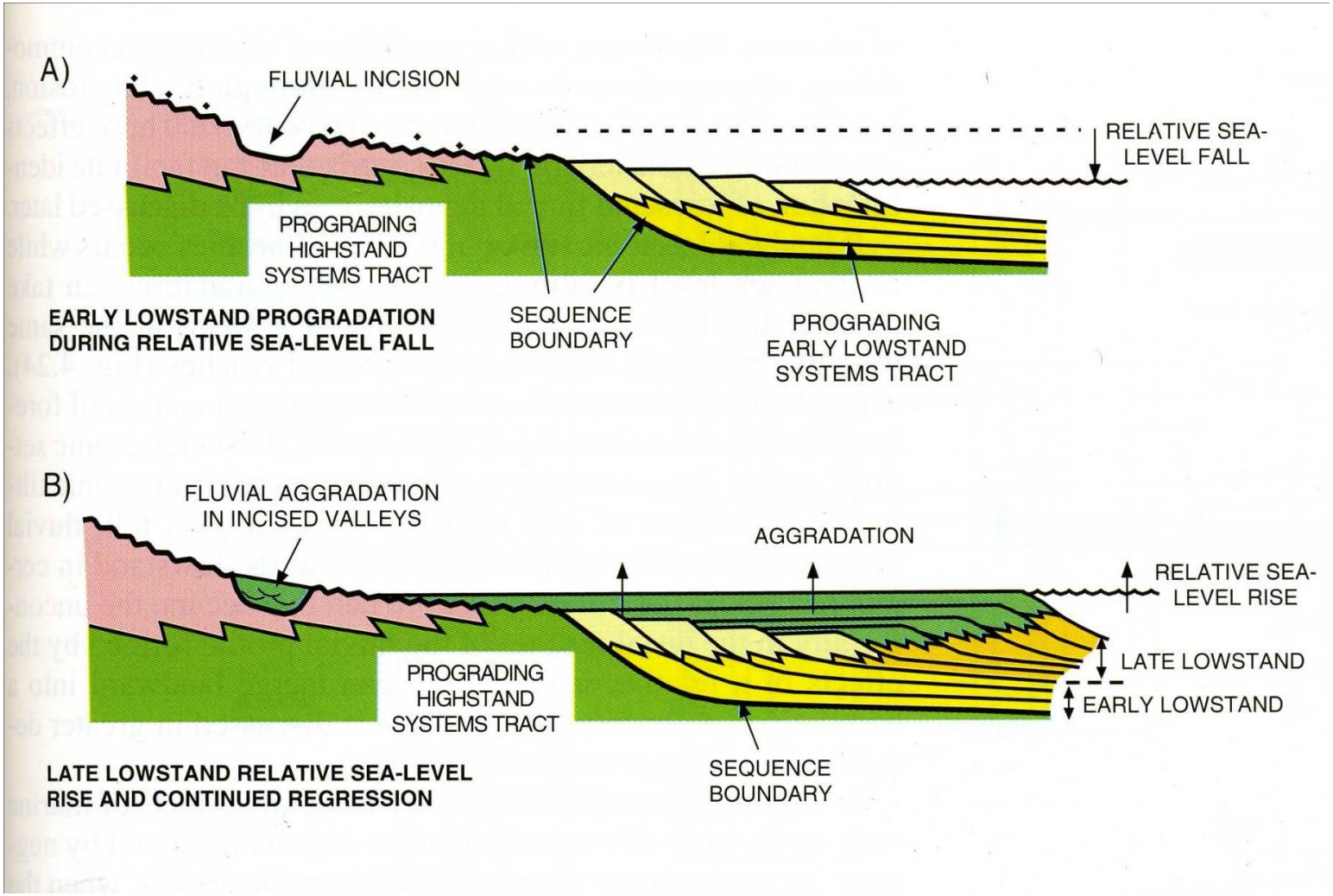

Figure 5.2. Sea-level fall in the figure above produces erosional unconformities which will be overlain by amalgamated sand bodies. Sea-level rise in the figure below results in aggradation and the deposition of muddier sediments (Posamentier and Allen, 1999).

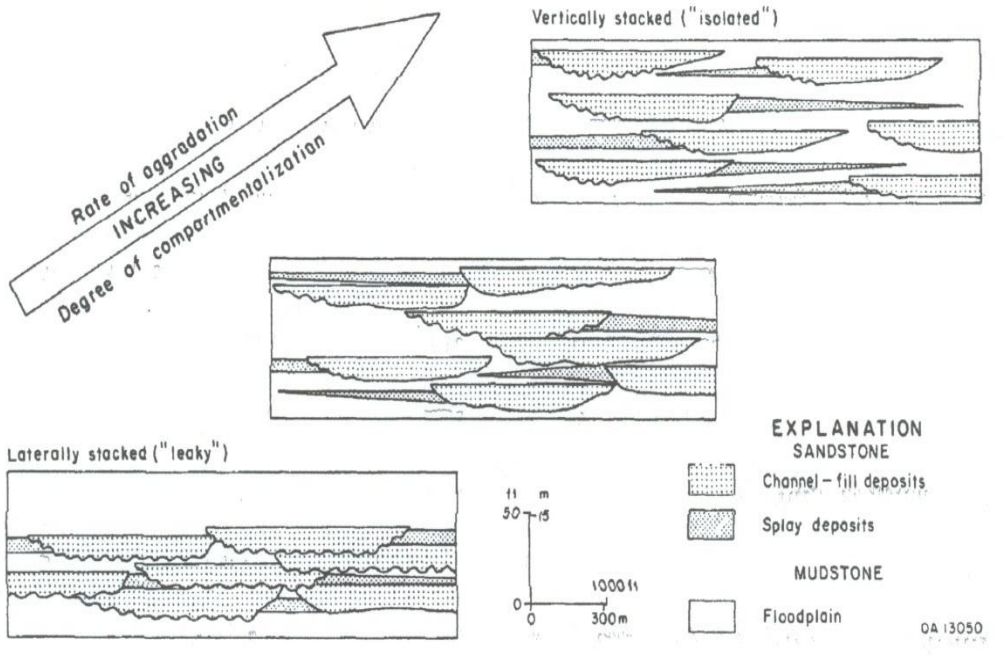

Figure 5.3. Aggradation rate affects mudstone preservation and therefore lithology. During low aggradation rates, mudstones are removed resulting in higher sand concentrations. Connectivity of sands is also influenced by aggradation rate, with a higher degree of compartmentalization associated with high aggradation rate and amalgamation of sands associated with low aggradation rate (modified from Kerr and Jirik, 1990).

deposition of a succession of progressively muddier sediments. As the cycle enters a regressive phase, the proportion of sand deposited begins to increase (Figure 5.4). Possible depositional sequences may be identified in the lithology depth curves generated for this study (Figure 5.5)

Therefore, it is reasonable to conclude that USGS-designated aquifer sands are a series of interconnected and amalgamated sand bodies deposited during times of low sediment aggradation associated with sea-level falling-stage system tracts and lowstand. The high degree of lateral connectivity allows these sands to act hydraulically as single units. It is also reasonable to infer that deposition of the mudstones that serve as confining units in the Baton Rouge aquifer system occurred during periods of relatively high aggradation rate which caused reduced vertical connectivity between sand-rich zones and is associated with sea-level highstand.

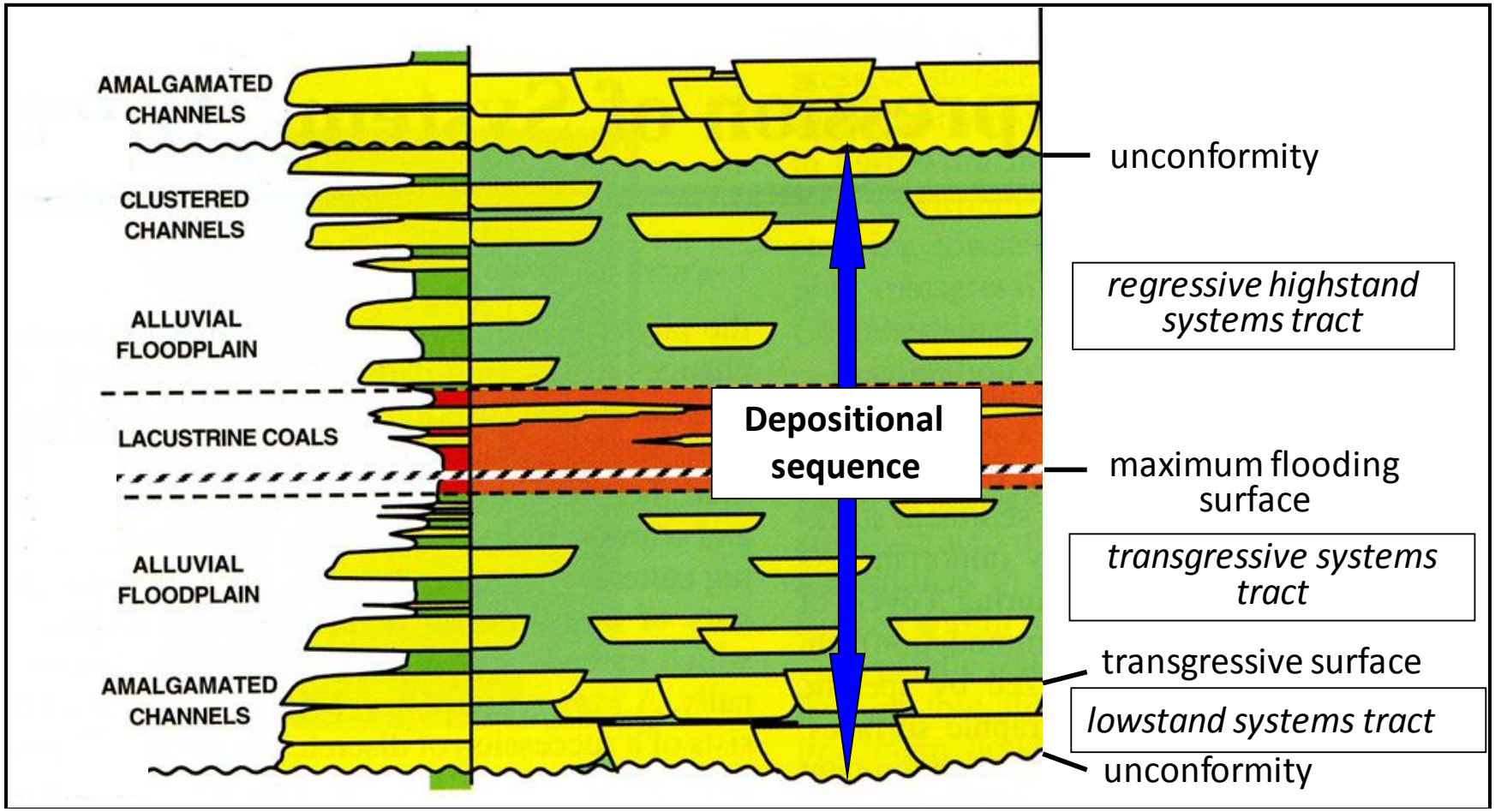

Figure 5.4. A fluvial depositional sequence starts with amalgamated sand (yellow) channels overlying an unconformity at the base, reflecting lowstand conditions following a drop in sea-level. As sea-level rises, a succession of progressively muddier (green) sediments is deposited. As the cycle enters a regressive phase, the proportion of sand begins to increase. The depositional sequence ends with a drop in sea-level and another erosional unconformity. Modified by Hanor from Posamentier and Allen (1999).

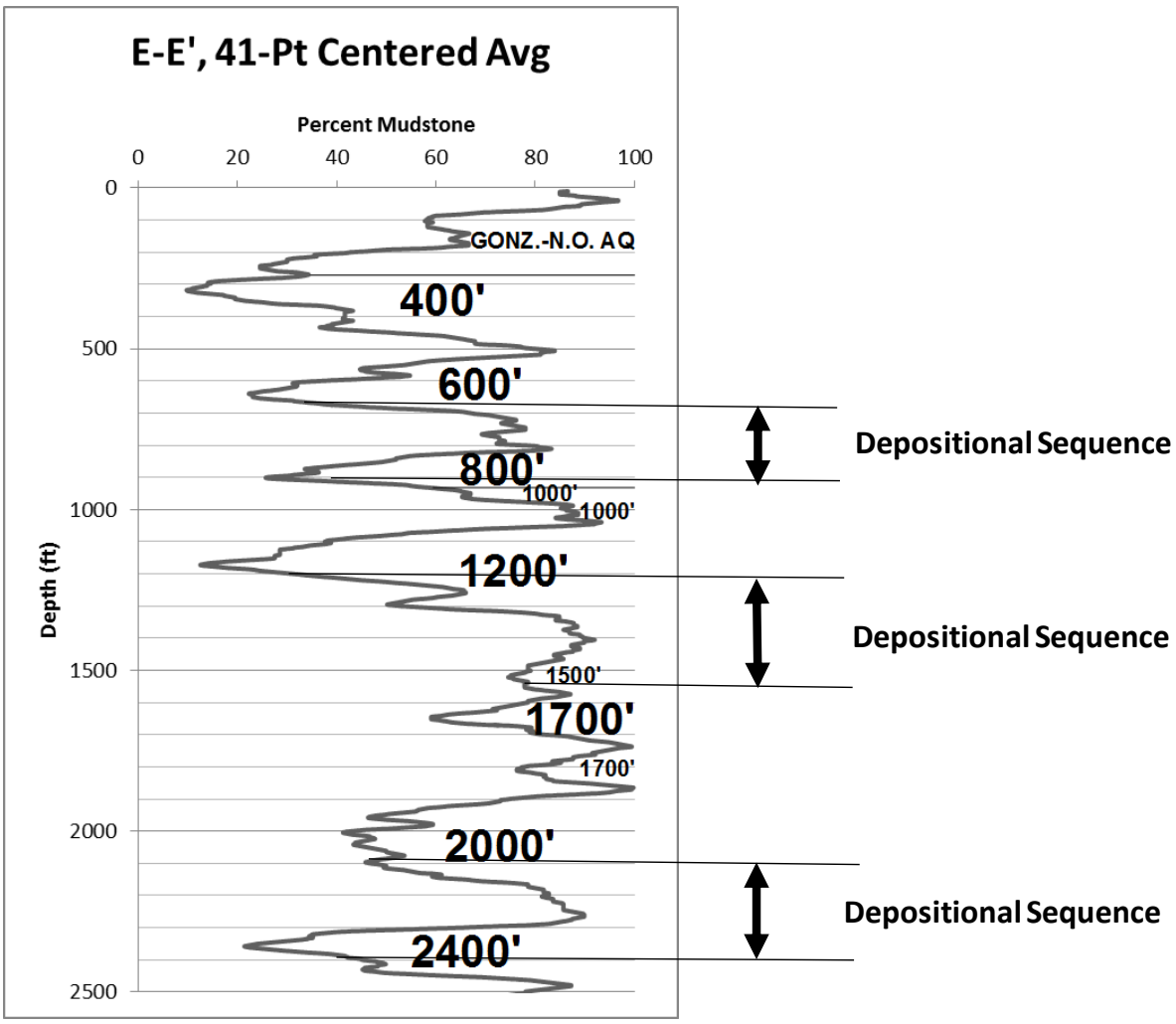

Figure 5.5. Identification of possible fluvial depositional sequences in the E-E' type section. Many more exist within this section. Note that the boundaries of the depositional sequences may lie toward the base of the sand-rich zones (Fig. 5.4).

The number of cycles identified in the lithology-depth curves was compared to the number of coastal onlap events shown in eustatic and relative Gulf of Mexico (GOM) coastal onlap curves. These curves were modified from sea-level curves by Styzen (1996) after Haq et al. (1988) (Figure 5.6). Relative sea-level differs from eustatic sea-level due to basin-specific sediment conditions (Hentz and Zeng, 2003). For example, modern relative Gulf of Mexico sea-level rise is greater than eustatic rise due to regional subsidence caused by sediment loading in the Gulf of Mexico (Day et al., 1995). Styzen's (1996) observed Gulf of Mexico relative coastal

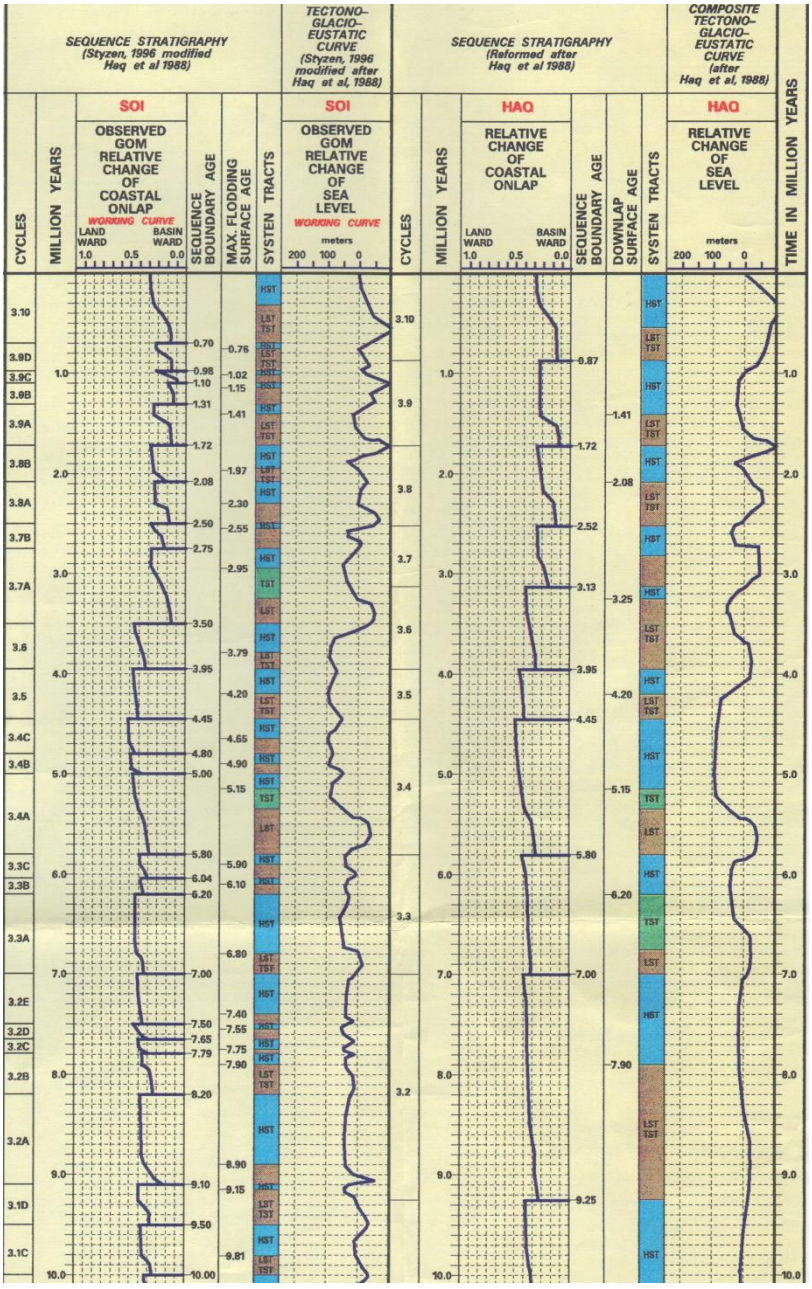

Figure 5.6. From left to right: relative Gulf of Mexico (GOM) coastal onlap curve, relative GOM sea-level curve, eustatic coastal onlap curve, and eustatic sea-level curve. Modified by Styzen (1996) after Haq (1988). The eustatic coastal onlap curve indicates 10 sea-level reversal events occurred from 10 Ma to present. The relative GOM coastal onlap curve shows 24 events for this same time period. Examples of high frequency, low amplitude events are seen at 5.0-4.6 Ma and 1.7-0.9 Ma in the relative GOM coastal onlap curve.

onlap curve recognized higher-order events than Haq et al. (1988), and documented 26 sea-level reversals in the northern Gulf of Mexico from 10 Ma to present. The eustatic coastal onlap curve modified from Haq et al. (1988) documented 10 reversal events within this same time period.

The 10 cycles identified in lithology-depth curves generated as part of this study match the number of cycles in the eustatic curve and have significantly fewer cycles than the 24 events indicated by the relative GOM coastal onlap curve by Styzen (1996) (Figure 5.6). This may be due to differences between fluvial and marine systems in sensitivity to forcing agents or sediment preservation. It is likely that high frequency, low amplitude reversals including those seen at 5.0-4.6 Ma and 1.7-0.9 Ma were not captured as large events in the geologic record, but may be the source of small signatures embedded within the sandy peaks of the lithology-depth curves. Additionally, fluvial systems may have lower sediment preservation than marine systems. Recent work in the Lower Mississippi River found sea-level influenced fluvial processes up to nearly 400 miles (600 km) upstream from the present shoreline (Shen et al., 2012). This suggests that the fluvial systems which deposited Baton Rouge aquifer sediments were sensitive to changes in relative sea-level but numerous and large unconformities in the study area have removed portions of the geologic record, which led to the preservation of fewer events than the 24 sea-level reversals identified in Styzen's (1996) relative GOM coastal onlap curve. Without more precise dating of the sediments, it is not possible to identify specific hiatuses or unconformities in the Baton Rouge aquifer system stratigraphic record.

6. CONCLUSIONS

6.1 Depositional environments of the Baton Rouge aquifer system

This study yielded the following conclusions:

- Sandy units of the Baton Rouge aquifer system were fluvially deposited and have highly complex geometries representing channel fill, floodplain, levee and crevasse splay facies. This is evident in well log-derived cross sections and three-dimensional renderings of the subsurface based on isometric fence diagrams.
- Lithology-depth curves support the USGS identification of individual hydraulic units separated by confining layers.
- These USGS-designated sands are best described as zones of amalgamated sand bodies. The amalgamation created a high degree of connectivity which causes these zones to behave hydraulically like single units.
- Cycles of sand-rich and mudstone-rich zones represent depositional sequences which were influenced by aggradation rate and forced by changes in relative Gulf of Mexico sea-level.
- Numerous and major unconformities in the study area have removed portions of the geologic record in the study area.

6.2 Applications of this study

This work resulted in the development of a process-based geologic framework for Baton Rouge aquifer sand bed geometries. The scientific knowledge gained from this study can be applied to environmental modeling efforts, thus contributing to ongoing mitigation of the threat of saltwater intrusion into freshwater aquifer sands. In addition, this work provides the first in-

depth geologic evaluation of depositional environments of Baton Rouge aquifer sediments, the first to utilize log response signatures since Heinrich's (1990) unpublished study.

6.3 Future work

Cross sections could be improved with the addition of constraints to the lateral extent of sand bodies. This could be done by mapping in area with a high density of well logs, such as an oil field. The lithology-depth curves for strike-oriented transects were a highly valuable tool in providing a quantitative assessment of depositional environments and could be successfully applied to future studies of sediments will well confined-dates to understand changes in aggradation rate and maybe ultimately inland sensitivity to sea-level change.

REFERENCES CITED

Blum, M.D., and Törnqvist, T.E. (2000) Fluvial responses to climate and sea-level change: a review and looking forward. Sedimentology, 47, 2-48.

Bray, R.B. and Hanor, J.S. (1990) Spatial variations in subsurface pore fluid properties in a portion of southeast Louisiana: Implications for regional fluid flow solute transport. Transactions- Gulf Coast Association of Geological Societies, 40, 53-64.

Buono, A. (1983) The Southern Hills regional aquifer system of southeastern Louisiana and southwestern Mississippi. USGS Water-Resources Investigations Report 83-4189. USGS, Baton Rouge, Louisiana, 38 pp.

Day, J.W., Pont, D., Hensel, P.F., Ibanez, C. (1995) Impacts of sea-level rise on deltas in the Gulf of Mexico and the Mediterranean: the importance of pulsing events to sustainability. Estuaries, 18, 4, 636-647.

Galloway, W.E. (1977) Catahoula Formation of the Texas Coastal Plain—depositional systems, composition, structural development, ground-water flow history, and uranium distribution. The University of Texas at Austin, Bureau of Economic Geology, Report of Investigations No. 87, 59.

Galloway, W.E. (2001) Cenozoic evolution of sediment accumulation in deltaic and shore-zone depositional systems, Northern Gulf of Mexico Basin. Marine and Petroleum Geology, 18, 1031-1040.

Galloway, W.E. (2005) Gulf of Mexico Basin depositional record of Cenozoic North American drainage basin evolution. Special Publications International Association of Sedimentologists, 35, 409-423.

Galloway, W. E., and Hobday, D. K. (1996) Terrigenous clastic depositional systems: Heidelberg, Springer-Verlag, 489 p.

Griffith, J.M. (2003) Hydrogeologic framework of southeastern Louisiana: Louisiana Department of Transportation and Development. Water Resources Technical Report No. 72, 14 Plates.

Hanor, J.S. (1971) Unpublished figures on the 3-D sand geometry, Baton Rouge Aquifer System.

Hanor, J.S. (1982) Reactivation of fault movement, Tepetate fault zone, south central Louisiana. Gulf Coast Association of Geological Societies, 32, 237-245.

Hanor, J.S., and Sassen, R. (1990) Large-scale vertical migration of formation waters, dissolved salt, and hydrocarbons in the Louisiana Gulf Coast, in D.Schumacher and B.F. Perkins, (ed.) Gulf Coast Oils and Gases, Their Characteristics, Origin, Distribution, and Exploration and

Production Significance: Proceedings 9th Annual Research Conference Gulf Coast Section, Society of Economic Paleontologists and Mineralogists, 283-296.

Haq, B.U., Hardenbol, J., and Vail, P.R. (1988) Mesozoic and Cenozoic chronostratigraphy and cycles of sea-level change, in C.K. Wilgus, C.A. Ross, H. Posamentier, and C.G. St. C. Kendall, eds., Sea-level changes: and integrated approach: SEMP Special Publication 42, 71-108.

Heinrich, P. V. (ca. 1990) Relationship of hydrogeology to depositional facies in the Baton Rouge, Louisiana aquifers. Unpublished report, Louisiana Geological Survey, 21 p.

Hentz, T.F., and Zeng, H. (2003) High-frequency Miocene sequence stratigraphy, offshore Louisiana: Cycle framework and influence on production distribution in a mature shelf province. American Association of Petroleum Geologists Bulletin, 87, 2, 197-230.

Kerr, D.R., and Jirik, L.A. (1990) Fluvial architecture and reservoir compartmentalization in the Oligocene Middle Frio formation, south Texas. Gulf Coast Association of Geological Societies, Transactions, 40, 373-380.

Li, X., and F. T.-C. Tsai. (2009) Bayesian model averaging for groundwater head prediction and uncertainty analysis using multimodel and multimethod. Water Resources Research, 45, W09403, doi:10.1029/2008WR007488.

Lovelace, J.K. (2007) Chloride concentrations in ground water in East and West Baton Rouge Parishes, Louisiana, 2004-05. Scientific Investigations Report 2007-5069.

Lovelace, J.K., and Lovelace, W.M. (1995) Hydrogeologic unit nomenclature and computer codes for aquifers and confining units in Louisiana, State of LA, Office of Public Works, Water Resources Special Report No. 9, 12.

Martin, A. and Whiteman, C.D. (1989) Geohydrology and regional ground-water flow of the coastal lowlands aquifer system in pats of Louisiana, Mississippi, Alabama, and Florida preliminary analysis. USGS Water Resources Investigations Report 88-4100, 88.

McCulloh, R.P., and Heinrich, P.V. (2012) Surface Faults of the South Louisiana Growth-Fault Province, in Cox, R.T., M. Tuttle, O. Boyd, and J. Locat, eds., Recent Advances in North American Paleoseismology and Neotectonics east of the Rockies and Use of the Data in Risk Assessment and Policy, Geological Society of America (in review).

McFarlan, E.Jr., and LeRoy, D.O. (1988) Subsurface geology of the late Tertiary and Quaternary deposits, coastal Louisiana and the adjacent continental shelf. Gulf Coast Association of Geological Societies Transactions, 38, 421-433.

Miall, A.D. (2010) Alluvial deposits. In: James, N. P., and Dalrymple, R. W., (ed.): Facies Models 4, pp. 105-137, Geological Association of Canada, St. John's, Newfoundland, 4th edition. GEOtext 6.

Miller, K. (2009) Sea-level change, last 250 million years, in V. Gornits, (ed.), Encyclopedia of Paleoclimatology and Ancient Environments, Springer Verlag, New York, 879-887.

Milliman, J.D. and Meade, R.H. (1983) Worldwide delivery of river sediment to the oceans. The Journal of Geology, 19, 1, 1-21.

Murray, G.E. (1947) Cenozoic deposits of central gulf coastal plain. American Association of Petroleum Geologists Bulletin, 31, 10, 1825-1850.

Pindell, J. and Dewey, J.F. (1982) Permo-Triassic reconstruction of western Pangea and the evolution of the Gulf of Mexico & sol; Caribbean region. Tectonics, 1, 2, 179-211. doi:10.1029/TC001i002p00179

Posamentier, H.W. and Allen, G.P. (1999) Facies and log expression of systems tracts. In: Dalrymple, R.W., Siliciclastic sequence stratigraphy- concepts and applications, pp. 103-121, SEPM Concepts in Sedimentology and Paleontology No. 7.

Roberts, H.H. (1997) Dynamic changes of the Holocene Mississippi River Delta plain: the delta cycle. Journal of Coastal Research, 13, 605–27.

Rollo, J.R. (1969) Saltwater encroachment in aquifers of the Baton Rouge Area, Louisiana: State of Louisiana. Office of Public Works, Water Resources Bulletin No. 13, 45.
Sargent, B.P. (2007) Water use in Louisiana, (2005). DOTD/USGS, Water Resources Special Report No. 16, 133.

Shen, Z., Törnqvist, T.E., Autin, W.J., Mateo, Z.R.P., Straub, K.M., and Mauz, B. (2012) Rapid and widespread response of the Lower Mississippi River to eustatic forcing during the last glacial-interglacial cycle. Geological Society of America Bulletin, 24 Feb 2012, doi:10.1130/B30449.1

Stoessell, R., and Prochaska, L. (2005) Chemical Evidence for Migration of Deep Formation Fluids into Shallow Aquifers in South Louisiana. Gulf Coast Association of Geological Societies Transactions, 55, 794-808.

Styzen, M.J., compiler. (1996) A chart in two sheets of the Late Cenozoic chronostratigraphy of the Gulf of Mexico. Gulf Coast Section SEMP Foundation.

Tsai, F.T.-C. (2010) Bayesian model averaging assessment on groundwater management under model structure uncertainty, Stochastic Environmental Research and Risk Assessment, 24, 845-861. doi:10.1007/s00477-010-0382-3.

Tsai, F. T.-C., and X. Li. (2008) Inverse groundwater modeling for hydraulic conductivity estimation using Bayesian model averaging and variance window. Water Resources Research 44(9), W09434, doi:10.1029/2007WR006576.

Wendeborn, C., and Hanor, J.S. (2008) The Baton Rouge Fault, South Louisiana: a barrier and/or conduit for vertical and/or lateral ground water flow? Baton Rouge Geological Society, Louisiana Groundwater and Water Resource Symposium, 26 Mar 2009.

Wright, L.D. and Coleman, J.M. (1973) Variations in morphology of major river deltas as functions of ocean wave and river discharge regimes. American Association of Petroleum Geologists Bulletin, 57, 370-398.

APPENDIX A: WELL LOG INFORMATION

Abbreviations:

NGVD29: National Geodetic Vertical Datum of 1929

PD: permanent datum

UNK: unknown

Table A.1. Information for well logs used in this study.

Well Designation in this Study	Well Use in this Study	Well Name	Well Type	UTM Coordinates	Date of Last Logging Run	Depth Interval (ft)	Log Datum Elev. above PD (ft)	Elev. above NGVD 29 (ft)	Source
S-1	S- Cross Section	Harry Laws No. 1	Oil	665425. 80 m E; 3364746. 47 m N; 15, N.	9/17/1979	128 - 10689	22	12	Wendeborn
S-2	S- Cross Section	Joe C. Reed #1	Oil	669722.00 m E; 3365475.49 m N; 15, N.	7/8/1956	0 - 10849	1	14	Wendeborn
S-3	S- Cross Section	USGS No. EB 783	USGS, EBR 783	673533 m E; 3366222 m N; 15, N.	5/8/1965	100 - 3011	3.5	26	Wendeborn
S-4	S- Cross Section	L. S. U. No. 1	Oil	675707.20 m E; 3366180.42 m N; 15, N.	6/26/1971	75 - 9516	17	30	Wendeborn
S-5	S- Cross Section	L. S. U. No. 1	Oil	680524.66 m E; 3364840.01 m N; 15, N.	5/30/1953	124 - 10503	17.12	40	Wendeborn
S-6	S- Cross Section	Ione Burden et al #1	Oil	681485.67 m E; 3365410.54 m N; 15, N.	8/28/1949	100 - 9420	15*	37	Wendeborn
S-7	S- Cross Section	D. E. McInnis #1	Oil	684120.05 m E; 3364224.18 m N; 15, N.	12/2/1939	1700 - 7501	15*	35	Wendeborn
S-8	S- Cross Section	USGS No. EB 803	USGS, EBR 803	688208 m E; 3366590 m N; 15, N.	2/7/1966	99 - 3202	2	27	Wendeborn
S-9	S- Cross Section	Lee Denham #1	Oil	693707.83 m E; 3361818.14 m N; 15, N.	1/24/1945	100 - 10294	15*	22	Wendeborn
S-10	S- Cross Section	Oliver A. Stevens A-1	Oil	696962.11 m E; 3361566.15 m N; 15, N.	5/7/1957	1850 - 10262	12.6	10	Wendeborn
S-11	S- Cross Section	J. Burton LeBlanc et al No. 1	Oil	69852.40 m E; 3361806.37 m N; 15, N.	6/24/1962	794 - 9734	14.9	21	Wendeborn
N-1	N-Cross Section	M. J. Kahao et al #1	Oil	663773.06 m E; 3373776.52 m N; 15, N.	11/21/1952	122 - 9527	16.4	21	Wendeborn
N-2	N-Cross Section	UGSG WBR No. 102	USGS, WBR 102	664108 m E; 3371742 m N; 15, N.	3/25/1966	82 - 2930	2.5	18	Wendeborn
N-3	N-Cross Section	USGS WBR No. 104	USGS, WBR 104	670246 m E; 3369897 m N; 15, N.	6/3/1966	79 - 2792	3	22	Wendeborn
N-4	N-Cross Section	W. B. R. No. 100	USGS, WBR 100	672416 m E; 3369315 m N; 15, N.	1/17/1966	60 - 2800	3	29	Wendeborn
N-5	N-Cross Section	USGS No. EB 794	USGS, EBR 794	675202 m E; 338026 m N; 15, N.	7/23/1965	100 - 2764	3.5	45	Wendeborn

Table A.1. Continued.

N-6	N-Cross Section	USGS EB 807	USGS, EBR 807	67330 m E; 3368430 m N; 15, N.	4/28/1966	80 - 2865	2.0	32	Wendeborn
N-7	N-Cross Section	USGS No. EB 790	USGS, EBR 790	679101 m E; 3368435 m N; 15, N.	6/17/1965	100 - 2803	4	45	Wendeborn
N-8, EBR 804	N-Cross Section, Block Diagram	USGS No. EB 804	USGS, EBR 804	685972.32 m E; 3365583.77 m N; 15, N.	2/22/1966	100 - 2861	3	46	Wendeborn
50039	Block Diagram	50039	DNR	662100.72 m E; 3374527.34 m N; 15, N.	12/1/1976	0 - 8770	15*	UNK	Tsai
WBR 101	Block Diagram	USGS No. WBR 101	USGS, WBR 101	668154 m E; 3370572 m N; 15, N.	4/5/1966	0 - 2973	5#	19	Tsai
EBR 806	Block Diagram	USGS No. EBR 806	USGS, EBR 806	674994 m E; 3369941 m N; 15, N.	4/20/1966	0 - 2943	5#	46.5	Tsai
EBR 790	Block Diagram	USGS No. EBR 790	USGS, EBR 790	679105 m E; 3368253 m N; 15, N.	6/17/1965	0 - 2804	4	45	Tsai
LI 56	Block Diagram	USGS No. LI 56	USGS, LI 56	5986694 m E; 3370395 m N; 15, N.	5/17/1955	0 - 2566	5#	40	Lovelace
A-1	A-A' Transect	033-850	USGS, EBR 850	664732.02 m E; 3393018.87 m N; 15, N.	10/28/1966	72 - 2442	4	95	Tsai
A-2	A-A' Transect	033-1174	USGS, EBR 1174	665644.16 m E; 3392570.92 m N; 15, N.	11/23/1987	1 to 2490	5#	90	Tsai
A-3	A-A' Transect	033-1186	USGS, EBR 1186	673133.24 m E; 3393797.47 m N; 15, N.	10/12/1988	85 - 2424	5#	95	Tsai
A-4	A-A' Transect	033-854	USGS, EBR 854	674116.60 m E; 3393905.73 m N; 15, N.	3/28/1968	0 - 2138	2.5	100	Tsai
A-5	A-A' Transect	033-770	USGS, EBR 770	677956.04 m E; 3391966.62 m N; 15, N.	7/17/1963	260 - 2192	7	97	Tsai
A-6	A-A' Transect	033-830	USGS, EBR 830	685029.71 m E; 3391007.85 m N; 15, N.	4/6/1967	395 - 2211	6	50	Tsai
A-7	A-A' Transect	033-832	USGS, EBR 832	694180.86 m E; 3393109.45 m N; 15, N.	6/11/1967	392 - 2042	3	88	Tsai
B-1	B-B' Transect	129-129	USGS, WBR 129	658517.72 m E; 3386520.25 m N; 15, N.	2/7/1975	20 - 2620	5#	29	Tsai
B-2	B-B' Transect	033-1314	USGS, EBR 1314	667045.40 m E; 3386340.88 m N; 15, N.	4/26/2002	1.5 - 2122.9	5#	81	Tsai

Table A.1. Continued.

B-3	B-B' Transect	033-645	USGS, EBR 645	669254.63 m E; 3384773.87 m N; 15, N.	10/31/1957	440 - 2632	3	80	Tsai
B-4	B-B' Transect	033-1001	USGS, EBR 1001	671842.12 m E; 3384599.16 m N; 15, N.	10/21/1976	90 - 1986	5#	68	Tsai
B-5	B-B' Transect	033-754	USGS, EBR 754	676924.31 m E; 3386683.12 m N; 15, N.	3/14/1963	46 - 2412	4	78	Tsai
B-6	B-B' Transect	033-892A	USGS, EBR 892	678752.77 m E; 3384064.60 m N; 15, N.	9/1/1972	24 - 2504	5	70	Tsai
B-7	B-B' Transect	033-1258	USGS, EBR 1258	687247.59 m E; 3384454.96 m N; 15, N.	11/7/1993	0 - 2100	5#	65	Tsai
B-8	B-B' Transect	033-1031	USGS, EBR 1031	690334.92 m E; 3386202.97 m N; 15, N.	11/8/1980	38 - 1991	5#	73	Tsai
B-9	B-B' Transect	033-581	USGS, EBR 581	692656.08 m E; 3384550.11 m N; 15, N.	4/11/1956	73 - 2595	5#	67	Tsai
B-10	B-B' Transect	063-323	USGS, LI 323	696253.69 m E; 3383105.64 m N; 15, N.	6/18/1999	0 - 2413	5#	62	Tsai
B-11	B-B' Transect	063-339	USGS, LI 339	698289.75 m E; 3385452.99 m N; 15, N.	2/5/2001	0 - 2068	5#	67	Tsai
C-1	C-C' Transect	154087	DNR	656192.47 m E; 3380781.97 m N; 15, N.	11/1/1976	100 - 3090	5#	20	Tsai
C-2	C-C' Transect	164740	DNR	665986.17 m E; 3381292.10 m N; 15, N.	8/10/1979	200 - 3130	5#	30	Tsai
C-3	C-C' Transect	033-1268	USGS, EBR 1268	671640.52 m E; 3382193.79 m N; 15, N.	9/14/1995	0 - 2632	5#	74	Tsai
C-4	C-C' Transect	033-572	USGS, EBR 572	672452.2 m E; 3381436.78 m N; 15, N.	2/18/1955	0 - 2584	3	71.5	Tsai
C-5	C-C' Transect	033-1000	USGS, EBR 1000	672914.58 m E; 3380859.02 m N; 15, N.	12/14/1977	50 - 3029	5#	68	Tsai
C-6	C-C' Transect	033-859	USGS, EBR 859	674556.93 m E; 3381501.37 m N; 15, N.	8/10/1967	125 - 2443	6	70	Tsai
C-7	C-C' Transect	033-1187	USGS, EBR 1187	676500.76 m E; 3381625.33 m N; 15, N.	1/10/1989	1 to 2552	5#	68.5	Tsai
C-8	C-C' Transect	033-1306	USGS, EBR 1306	689846.82 m E; 3380619.50 m N; 15, N.	11/21/2000	0 - 2183	5#	57	Tsai
C-9	C-C' Transect	063-307	USGS, LI 307	695703.71 m E; 3381093.57 m N; 15, N.	11/22/1996	0 - 2115	5#	55	Tsai

Table A.1. Continued.

D-1	D-D' Transect	159088	DNR	658461.57 m E; 3378940.49 m N; 15, N.	4/20/1978	304 - 3004	5#	20	Tsai
D-2	D-D' Transect	156290	DNR	662128.90 m E; 3379693.91 m N; 15, N.	7/15/1977	150 - 3030	5#	17	Tsai
D-3	D-D' Transect	033-812	USGS, EBR 812	672514.71 m E; 3379189.59 m N; 15, N.	3/29/1961	400 - 2022	6	65	Tsai
D-4	D-D' Transect	033-750	USGS, EBR 750	673002.36 m E; 3378704.63 m N; 15, N.	9/9/1962	400 - 2646	2	50	Tsai
D-5	D-D' Transect	033-798	USGS, EBR 798	675058.80 m E; 3378491.33 m N; 15, N.	5/22/1965	389 - 2697	5#	60	Tsai
D-6	D-D' Transect	033-1281	USGS, EBR 1281	685935.11 m E; 3378641.96 m N; 15, N.	2/19/1998	125 - 3030	9.5	91	Tsai
D-7	D-D' Transect	033-955	USGS, EBR 995	686081.27 m E; 3379445.26 m N; 15, N.	11/2/1976	550 - 2770	1	58	Tsai
D-8	D-D' Transect	033-1032	USGS, EBR 1032	691298.08 m E; 3376949.03 m N; 15, N.	7/28/1981	20 - 2343	5#	45	Tsai
E-1	E-E' Transect	121-134	USGS, WBR 134	654923.23 m E; 3373380.66 m N; 15, N.	9/25/1975	20 -2434	5#	12	Tsai
E-2	E-E' Transect	48418	DNR	662144.50 m E; 3374184.45 m N; 15, N.	4/7/1953	1020 - 3250	5#	20	Tsai
E-3	E-E' Transect	47052	DNR	663773.06 m E; 3373776.52 m N; 15, N.	12/1/1976	110 - 3275	5#	21	Tsai
E-4	E-E' Transect	41049	DNR	665762.31 m E; 3373673.57 m N; 15, N.	12/1/1976	100 - 3220	5#	23	Tsai
E-5	E-E' Transect	121-33	USGS, WBR 33	670084.63 m E; 3372653.06 m N; 15, N.	12/11/1953	90 - 3050	5#	25	Tsai
E-6	E-E' Transect	033-398	USGS, EBR 398	673933.96 m E; 3373822.82 m N; 15, N.	3/1/1958	30 - 2480	5#	50	Tsai
E-7	E-E' Transect	033-884	USGS, EBR 884	675479.67 m E; 3373909.33 m N; 15, N.	7/25/1969	50 - 2429	4	65	Tsai
E-8	E-E' Transect	033-1303	USGS, EBR 1303	682914.033 m E; 3373909.33 m N; 15, N.	12/15/1999	83 - 2643	7.5	45	Tsai
E-9	E-E' Transect	033-926	USGS, EBR 926	686143.56 m E; 3374272.04 m N; 15, N.	2/23/1973	20 - 2640	2	50	Tsai
E-10	E-E' Transect	033-1262	USGS, EBR 1262	690011.79 m E; 3372737.57 m N; 15, N.	8/2/1994	0 - 2636	5#	47	Tsai

Table A.1. Continued.

E-11	E-E' Transect	063-153	USGS, LI 153	695782.40 m E; 3373795.09 m N; 15, N.	3/3/1972	20 - 2716	5[#]	42	Tsai
E-12	E-E' Transect	063-302	USGS, LI 302	696465.21 m E; 3374392.68 m N; 15, N.	2/12/1994	0 - 2474	5[#]	40	Tsai
E-13	E-E' Transect	063-181	USGS, LI 181	697753.18 m E; 3373984.89 m N; 15, N.	1/17/1978	140 - 2675	6	31	Tsai
E-14	E-E' Transect	063-266	USGS, LI 266	698925.52 m E; 3374067.95 m N; 15, N.	8/3/1989	173 - 2471	5	30	Tsai
* UNK. Average datum for oil wells assumed to be 15 ft.									
[#] UNK. Average datum for water wells assumed to be 5 ft.									

APPENDIX B: LITHOLOGY-DEPTH CURVES

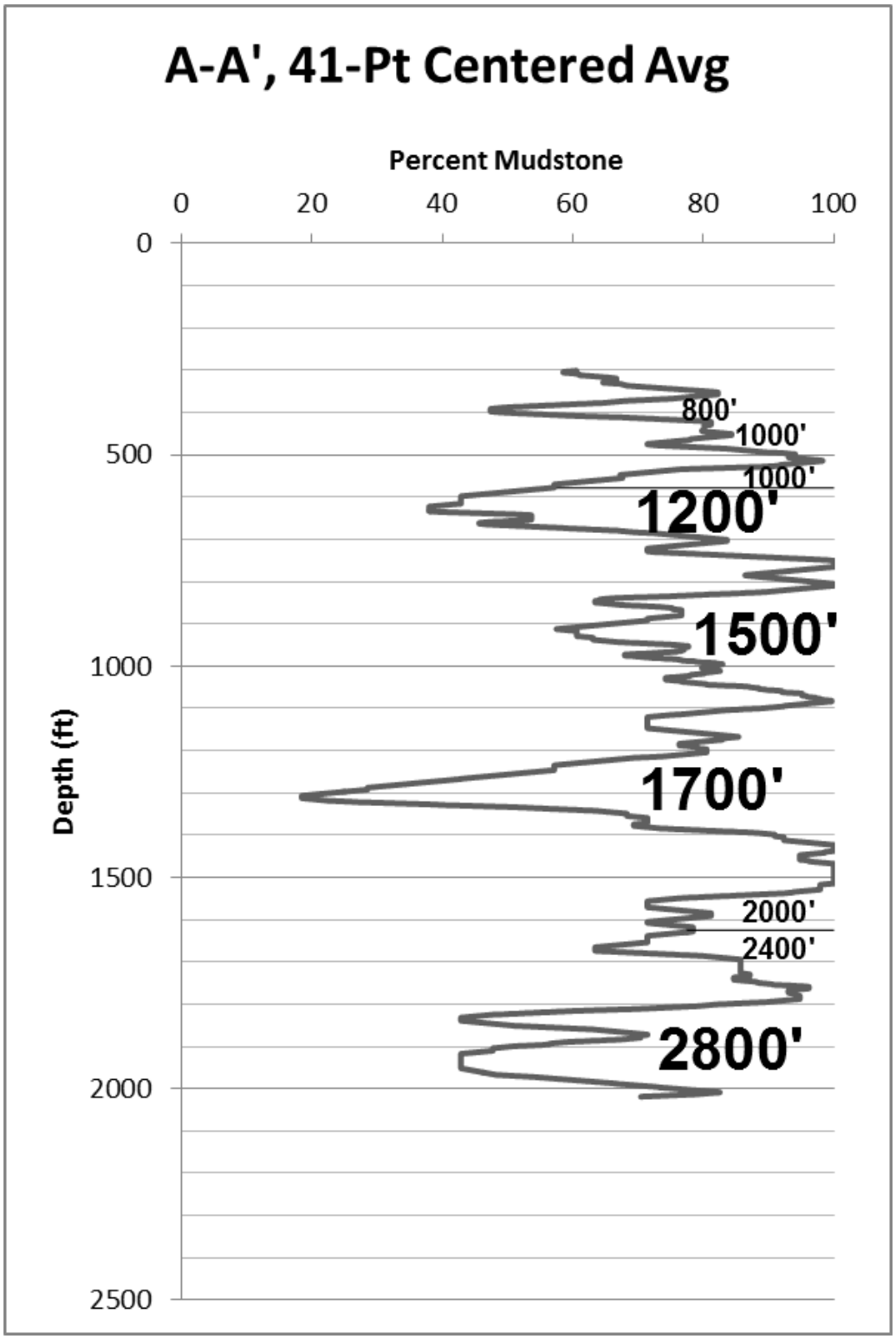

Figure B.1. Lithology-depth curve for transect A-A'. Sand peaks are labeled with correlated USGS-designated aquifer units.

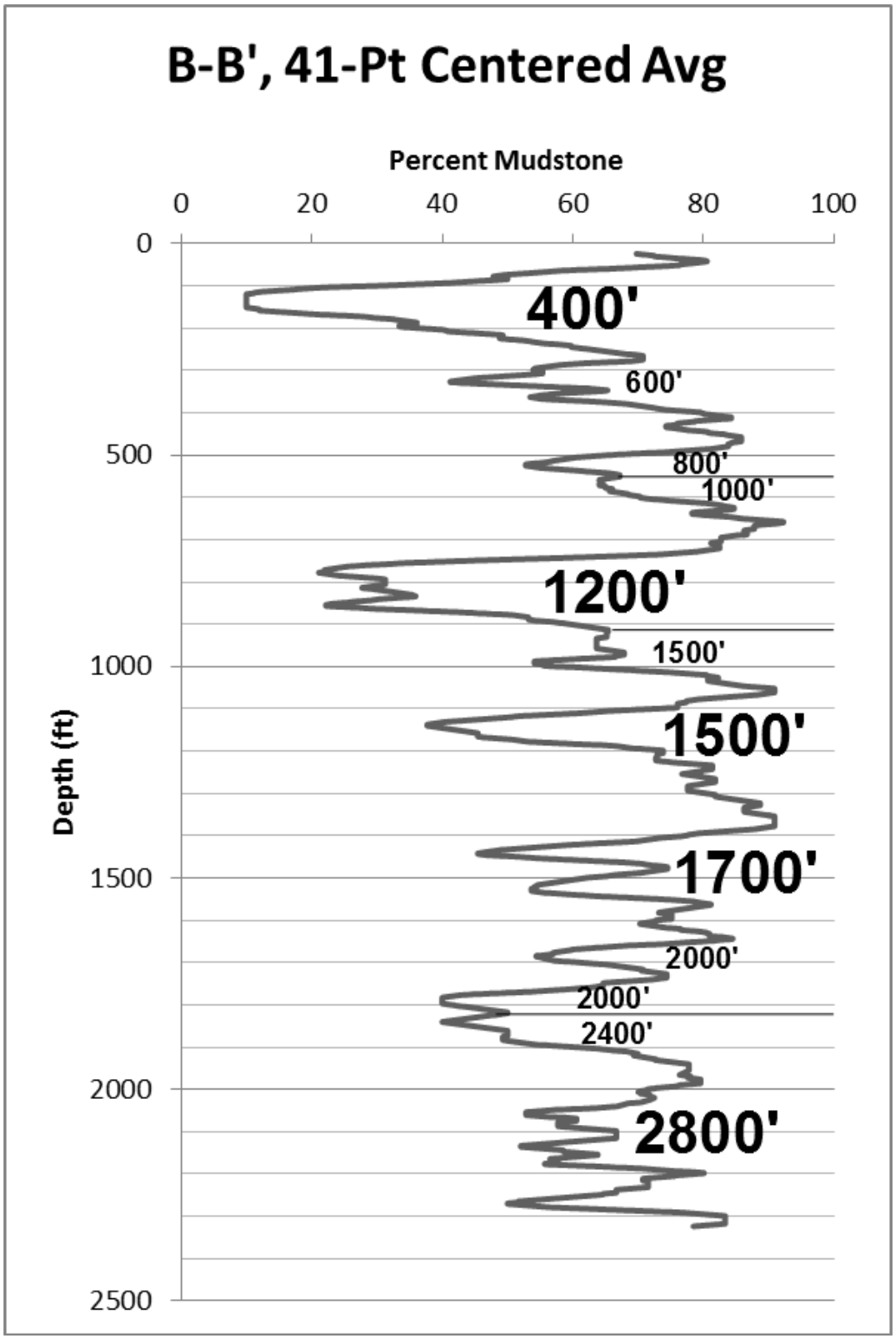

Figure B.2. Lithology-depth curve for transect B-B'. Sand peaks are labeled with correlated USGS-designated aquifer units.

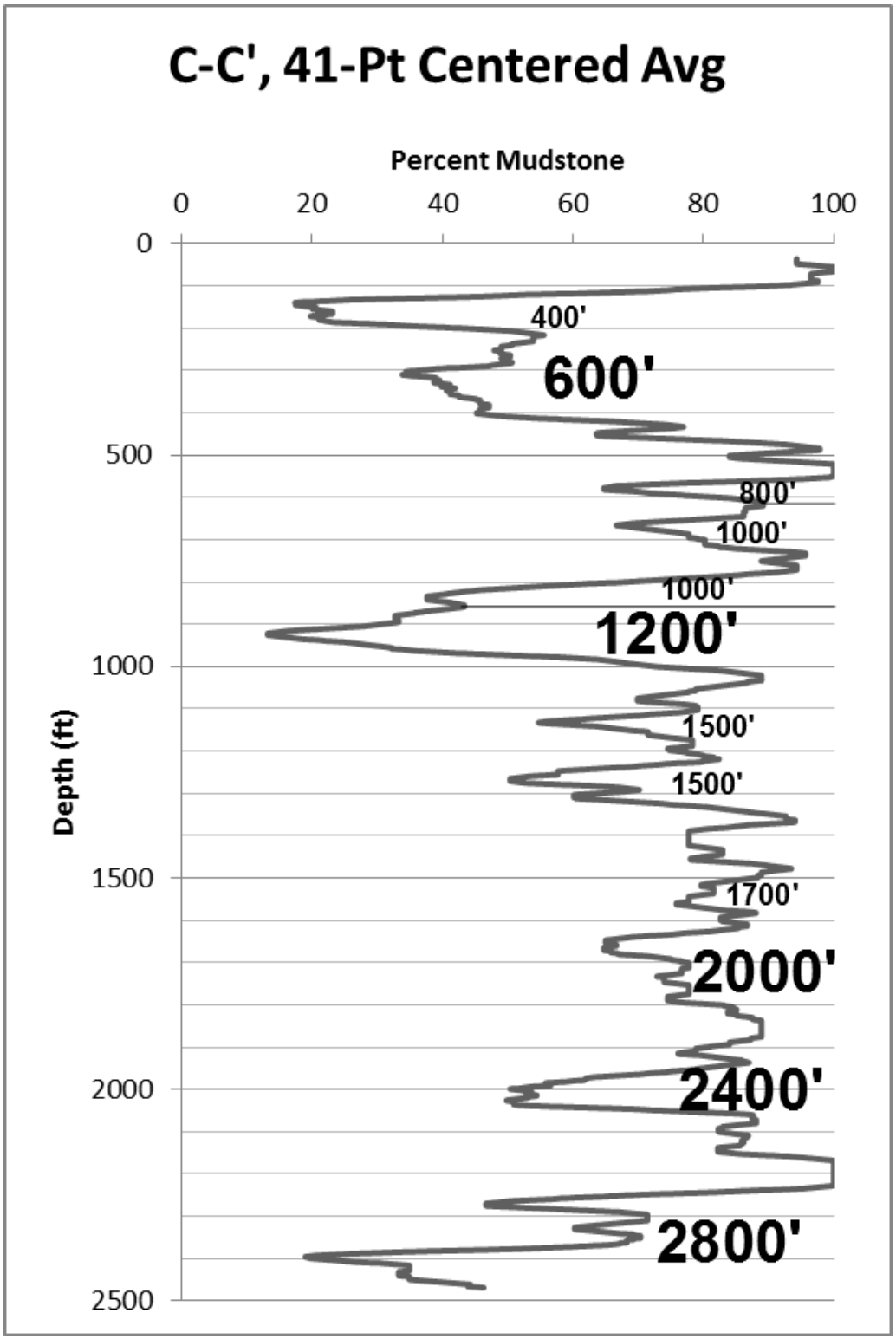

Figure B.3. Lithology-depth curve for transect C-C'. Sand peaks are labeled with correlated USGS-designated aquifer units.

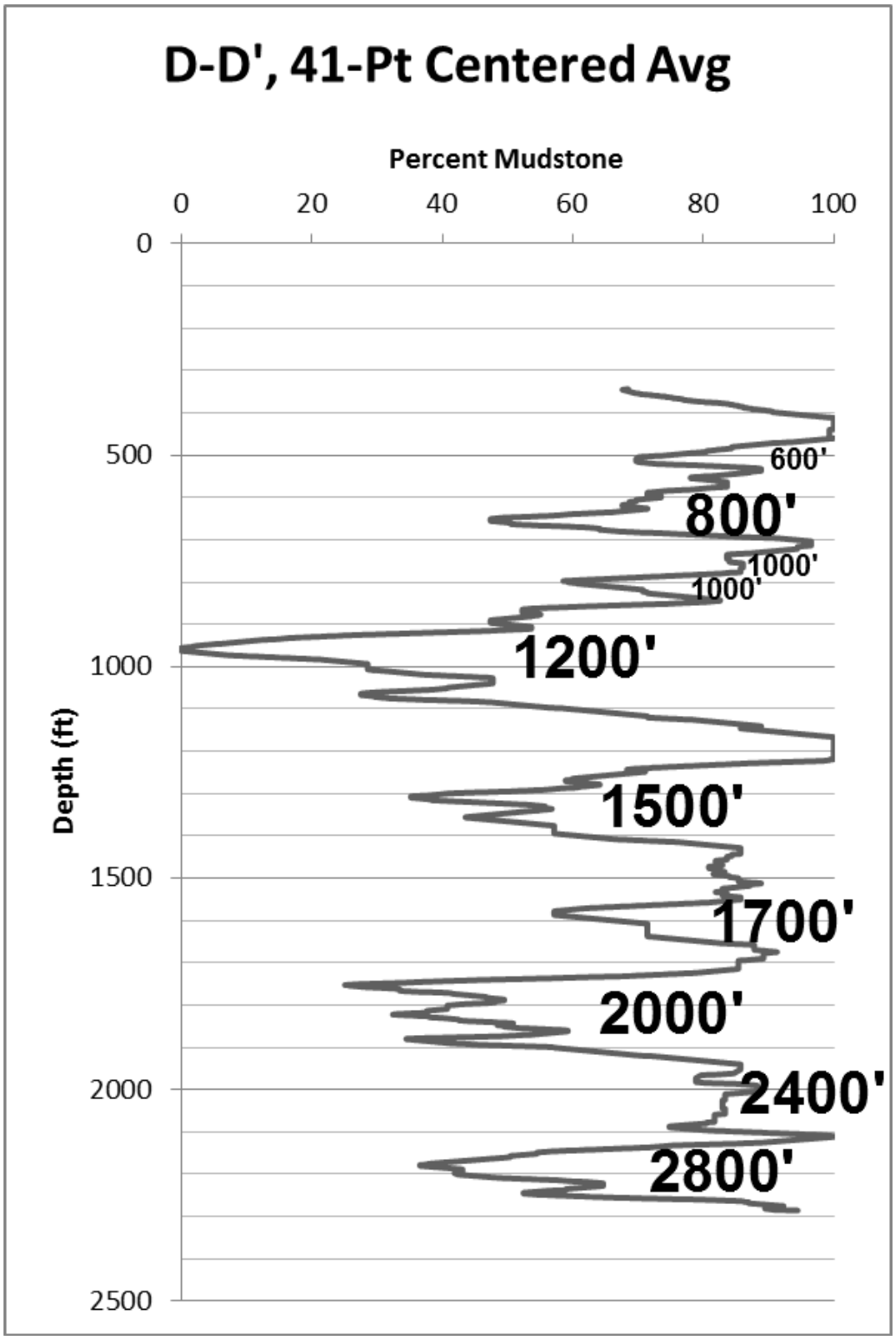

Figure B.4. Lithology-depth curve for transect D-D'. Sand peaks are labeled with correlated USGS-designated aquifer units.

VITA

Elizabeth Laurel Chamberlain graduated as valedictorian and a National Merit Scholar from Palmyra Eagle High School. She left her home-state of Wisconsin in 2002 to pursue a pre-veterinary program at Louisiana State University, Baton Rouge, Louisiana. There, Elizabeth also studied lithography and creative writing. She soon learned that animals do gross things. Sediments do not do these things. After earning a B.S in Animal Science, B.A. in Liberal Arts and B.A. in English in 2007, Elizabeth moved to New Orleans where she pursued odd jobs. Throughout her time in south Louisiana, Elizabeth been fascinated by the powerful Mississippi River which shapes the local landscape. Elizabeth continued her studies in 2010, applying her passion for science to the field of geology. She will earn a M.S. in Geology from Louisiana State University in August, 2012. Elizabeth plans to pursue a PhD in Earth and Environmental Sciences at Tulane University beginning in the fall of 2012.